J Physiol (2003), **547.3**, *pp.* 873–891
DOI: 10.1113/jphysiol.2002.036434

www.jphysiol.org

Journal of Physiology

Cl^- flux through a non-selective, stretch-sensitive conductance influences the outer hair cell motor of the guinea-pig

Volodymyr Rybalchenko and Joseph Santos-Sacchi

Departments of Surgery (Otolaryngology) and Neurobiology, Yale University School of Medicine, 333 Cedar Street, New Haven, CT 06510, USA

Outer hair cells underlie high frequency cochlear amplification in mammals. Fast somatic motility can be driven by voltage-dependent conformational changes in the motor protein, prestin, which resides exclusively within lateral plasma membrane of the cell. Yet, how a voltage-driven motor could contribute to high frequency amplification, despite the low-pass membrane filter of the cell, remains an enigma. The recent identification of prestin's Cl^- sensitivity revealed an alternative mechanism in which intracellular Cl^- fluctuations near prestin could influence the motor. We report the existence of a stretch-sensitive conductance within the lateral membrane that passes anions and cations and is gated at acoustic rates. The resultant intracellular Cl^- oscillations near prestin may drive motor protein transitions, as evidenced by pronounced shifts in prestin's state-probability function along the voltage axis. The sensitivity of prestin's state probability to intracellular Cl^- levels betokens a more complicated role for Cl^- than a simple extrinsic voltage sensor. Instead, we suggest an allosteric modulation of prestin by Cl^- and other anions. Finally, we hypothesize that prestin sensitivity to anion flux through the mechanically activated lateral membrane can provide a driving force that circumvents the membrane's low-pass filter, thus permitting amplification at high acoustic frequencies.

(Resubmitted 22 November 2002; accepted after revision 18 December 2002; first published online 31 January 2003)
Corresponding author J. Santos-Sacchi: Department of Surgery (Otolaryngology), BML 244, Yale University School of Medicine, 333 Cedar Street, New Haven, CT 06510, USA. Email: joseph.santos-sacchi@yale.edu

The mammalian outer hair cell (OHC) evolved from more primitive hair cells, such as its counterpart, the inner hair cell (IHC), to enhance detection and discrimination of high frequency sounds (Dallos, 1992). A key evolutionary step appears to have been the recruitment of an anion transporter family member, prestin (Zheng *et al.* 2000), to transform the cell into an effector as well as sensor, capable of boosting passive basilar membrane motion (Liberman *et al.* 2002). Electrical stimulation evokes rapid length changes in OHCs (Brownell *et al.* 1985; Kachar *et al.* 1986), which possibly result from membrane surface area changes caused by conformational transitions in the integral membrane motor protein (Kalinec *et al.* 1992; Santos-Sacchi, 1993; Iwasa, 1994; Santos-Sacchi & Navarrete, 2002). The mechanism displays a sigmoidal voltage dependence (Ashmore, 1987; Santos-Sacchi & Dilger, 1988), resides exclusively in the OHC lateral plasma membrane (Dallos *et al.* 1991; Huang & Santos-Sacchi, 1993; Takahashi & Santos-Sacchi, 2001) and shows reciprocal sensitivity to membrane voltage and tension (Iwasa, 1993; Gale & Ashmore, 1994; Kakehata & Santos-Sacchi, 1995; Ludwig *et al.* 2001; Santos-Sacchi *et al.* 2001). The electrical signature of the motor protein is its displacement current, or an equivalent bell-shaped, voltage-dependent capacitance owing to its voltage sensor's charge movement within and normal to the plane of the lateral plasma membrane (Ashmore, 1990; Santos-Sacchi, 1991*b*). The probability of the motor being in a contracted or expanded state (referred to as state probability hereafter) can be determined from capacitance *vs.* voltage (*C*–*V*) functions.

Initial work on electromotility indicated that it was driven by transmembrane potassium current (Ashmore, 1986; Ashmore & Meech, 1986). Subsequently, evidence accumulated showing that the phenomenon was voltage dependent (Santos-Sacchi & Dilger, 1988; Ashmore, 1989; Iwasa & Kachar, 1989; Santos-Sacchi, 1992). This observation coupled to the finding that the gain of the mechanical response is less than maximal near the OHC's normal resting potential, led to the realization that the resistance–capacitance (RC) membrane filter would seriously limit the driving force for electromotility at high frequencies (Santos-Sacchi, 1989, 1992). But, in fact, the high frequency region is where the cochlear amplifier is most effective (Ruggero & Rich, 1991). Thus, although the prestin-based motor mechanism can be driven by experimentally

applied voltage sources at very high frequencies (> 70 kHz (Frank *et al.* 1999)), the problem remains that receptor potentials in the OHC are attenuated at 6 db octave^{-1} above the cell's RC cut-off frequency (Dallos & Santos-Sacchi, 1983). The recent discovery of the intracellular Cl^- sensitivity of prestin (Oliver *et al.* 2001) revealed a possible alternative mechanism where a hypothetical transmembrane Cl^- current could affect prestin activity. We report here the existence of an OHC conductance that is Cl^- permeable, and mechanically gated at high frequencies. Spatially co-located with prestin to the lateral plasma membrane, this conductance results in changes in intracellular Cl^- concentration near prestin that drive motor protein transitions and, consequently, OHC mechanical activity. Thus, we hypothesize that a mechanically gated ionic current, which is intrinsically unaffected by the membrane time constant τ, could provide the driving force for the cochlear amplifier.

METHODS

General

Guinea-pigs were killed with halothane inhalation overdose in accordance with an approved protocol from Yale University's animal use and care committee. OHCs were freshly isolated from the adult guinea-pig organ of Corti by sequential enzymatic (dispase 0.5 mg ml^{-1}) and mechanical treatment in Ca^{2+}-free medium. Currents from voltage-clamped cells were recorded at room temperature using an Axon 200B amplifier, Digidata 1231A board (Axon Instruments, CA, USA) and the software program jCLAMP (Scisoft, CT, USA). The major intracellular and extracellular solutions are listed in Tables 1 and 2. At the ion concentrations listed, pH was 7.25–7.30; the osmolality was ~325 mosmol kg^{-1} for extracellular solutions, and ~5 mosmol kg^{-1} lower for intracellular solutions to prevent swelling.

In some cases we added $CdSO_4$ (1 mM) to block Ca^{2+} currents. When evaluating K^+ ions, 4-aminopyridine (4-AP; 1 mM) and linopirdine (200 μM) were used to block K^+ channels. Solutions were delivered to individual cells by Y tube, during continuous whole-bath perfusion with Tris-Hepes solution. Series resistance (before correction off-line) was ~7–20 MΩ in Tris-Hepes solution. A combined Ag–AgCl–KCl–K_2SO_4-agar ground electrode maintained liquid junction potentials in the range ±1–2 mV during solution exchanges. Up to 1% DMSO used in extracellular solutions for dissolution of tested pharmacological agents had no influence on the membrane resistance, capacitance or ionic currents. All chemicals were from Sigma (MO, USA) or Fluka (Switzerland). Data are presented as means ± S.E.M.

Measurement of non-linear capacitance

Non-linear membrane capacitance was evaluated using a continuous high resolution (2.56 ms sampling) two-sine voltage stimulus protocol (10 mV peak at both 390.6 and 781.2 Hz), with subsequent fast Fourier transform-based admittance analysis as fully described by Santos-Sacchi *et al.* (1998*b*). These high frequency sinusoids were superimposed on voltage ramps. Peak non-linear capacitance was determined by subtracting linear capacitance. *C–V* data were fitted with the first derivative of a two-state Boltzmann function and a constant representing the linear capacitance (Santos-Sacchi, 1991*b*):

$$C_m = Q_{max}\frac{ze}{kT}\frac{b}{(1+b)^2} + C_{lin}, \quad (1)$$

and

$$b = \exp\left(\frac{-ze(V_m - V_{pkcm})}{kT}\right),$$

where Q_{max} is the maximum non-linear charge moved, V_{pkcm} is voltage at peak capacitance or half-maximal non-linear charge transfer, V_m is membrane potential, C_{lin} is linear capacitance, z is apparent valence, e is electron charge, k is Boltzmann's constant and T is absolute temperature.

Mechanical stimulation of the lateral membrane

Three methods were used to mechanically stimulate the lateral membrane while recording whole-cell currents. In order to induce steady-state changes in membrane tension, positive or negative pressure into the cells was applied through the patch pipette and was monitored with an electronic pressure monitor. For step and low frequency stimulation, a piezoelectrically driven stiff glass probe was used to deform the cell near the mid region of the lateral membrane. The device was the same as that used previously to calibrate a photodiode displacement measurement technique (see Santos-Sacchi, 1992). The long axis of the probe was positioned parallel to the perfusion chamber bottom and normal to the longitudinal axis of the cell (see Fig. 11). OHCs were compressed statically and vertical DC or AC displacements of the probe (±2 μm) were superimposed. For high frequency stimulation, a closely positioned (15–20 μm) piezoelectric-driven fluid-jet pipette (5–10 μm tip diameter) was used as previously described (Takahashi & Santos-Sacchi, 2001). The pipette contained bath solution and was pointed perpendicular to the surface of the lateral membrane. The latter system is similar to that used previously (Brundin & Russell, 1994), although we used it simply to stimulate the lateral membrane and measure whole-cell currents. That is, we did not replicate their study. Care was taken to drive the piezoelectric only within its linear range, and use filters to limit driver resonances. Following dissociation of OHCs in Ca^{2+}-free medium, stereocilia were either fully absent or very badly damaged; thus there was no contribution from stereocilia to the mechanically generated currents we observed.

RESULTS

Intracellular dialysis of Cl^--free solution shifts prestin's voltage dependence with little effect on motor charge movement

In order to study the effects of Cl^- removal on the OHC motor, we used intracellular solutions that were either Tris-sulfate or Tris-Hepes based (Tables 1 and 2), as these solutes are expected to be neutral with respect to prestin activity (Oliver *et al.* 2001). The OHC presents a bell-shaped *C–V* function whose voltage at peak capacitance (V_{pkcm}) is highly susceptible to intracellular Cl^- washout following the establishment of whole-cell configuration, shifting in the depolarizing direction (Fig. 1). The degree of voltage shift and modulation of peak non-linear capacitance depends upon the species of control anion.

Figure 1*A* and *B* shows that, in the presence of 140 mM extracellular Cl^-, and after washout of intracellular Cl^- during whole-cell dialysis with Cl^--free patch pipette solutions, peak non-linear capacitance remained stable when the major intracellular anion was sulfate (steady state: 96.5 ± 5 % of initial value of 20.63 ± 1.12 pF; mean ± S.E.M.; $n = 5$). However, V_{pkcm} showed a very large positive shift from an initial value of −4.9 ± 2.7 to +97.4 ± 7.6 mV, reflecting a change in motor-state probability. On the other hand, washout with Tris-Hepes based, Cl^--free intracellular solutions decreased peak C_m to 75.3 ± 3.7 % at steady state (initial value: 19.53 ± 2.64 pF; $n = 4$), with a smaller V_{pkcm} shift from −24.4 ± 0.6 to +8.2 ± 3.5 mV.

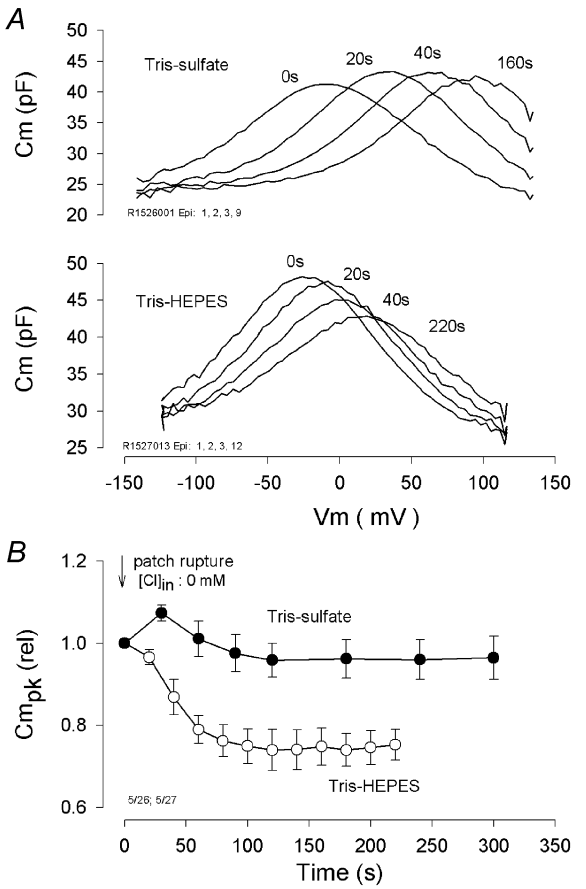

Figure 1. Effects of intracellular Cl^- on prestin-generated non-linear capacitance in outer hair cells (OHCs)

A, top, *C*–*V* functions of an OHC during washout of Cl^- with Tris-sulfate patch-pipette solution, in the presence of 140 mM Tris-Cl extracellular solution. Bottom, same as above except with Tris-Hepes pipette solution. *B*, relative peak non-linear capacitance (C_{mpk} (rel)) as a function of time after patch rupture with either Tris-sulfate ($n = 4$; mean ± S.E.M.) or Tris-Hepes ($n = 5$) Cl^--free intracellular solutions and Tris-Cl 140 mM (140 Cl) extracellular solution. Recordings began at the moment of patch rupture at a holding potential of 0 mV. Data were obtained from full *C*–*V* functions, and peak non-linear membrane capacitance C_m was obtained by subtracting linear capacitance determined by fits (see Methods) to the data. $[Cl]_{in}$, intracellular Cl^- concentration.

Since peak non-linear capacitance ($C_{mpk} = Q_{max}ze/4kT$) depends on slope (z) and Q_{max} of the charge–voltage (Q–V) relationship, the parameters describing the motor's charge movement were obtained by fitting (see Methods) OHC non-linear capacitance with the first derivative of a two-state Boltzmann function (Fig. 2). In addition to the large shifts in the operating voltage range, both the voltage sensitivity (z) and the maximum charge moved (Q_{max}) of the motor were affected by intracellular Cl^- removal; however, even in the steady state presence of Cl^--free intracellular solutions, Q_{max} remained greater than 80 % of initial values. Following the removal of extracellular Cl^-, Q_{max} remained robust, but its magnitude, as well as that of z, depended on the species of intracellular anion (SO_4^{2-} *vs.* Hepes; see Fig. 2). In order to assure ourselves that submembranous, intracellular Cl^- and other active anions, e.g. bicarbonate (Oliver *et al.* 2001), were depleted, we pretreated cells in a continuous wash of Tris-Hepes Cl^--free extracellular solutions for over 4 h prior to recording with Cl^--free patch-pipette solutions, a procedure that has been shown to rapidly deplete intracellular stores of Cl^- (Aickin & Brading, 1984; Thoreson *et al.* 2000). Even under these conditions, non-linear charge movement remained considerable (Tris-sulfate intracellular: Q_{max}, 0.99 ± 0.27 pC; z, 0.62 ± 0.07; V_{pkcm}, 141 ± 9 mV; C_{lin}, 22.9 ± 1.7 pF; $n = 5$; Tris-Hepes intracellular: Q_{max}, 1.45 ± 0.19 pC; z, 0.66 ± 0.02; V_{pkcm}, 57 ± 4 mV; C_{lin}, 24.6 ± 2.0 pF; $n = 5$).

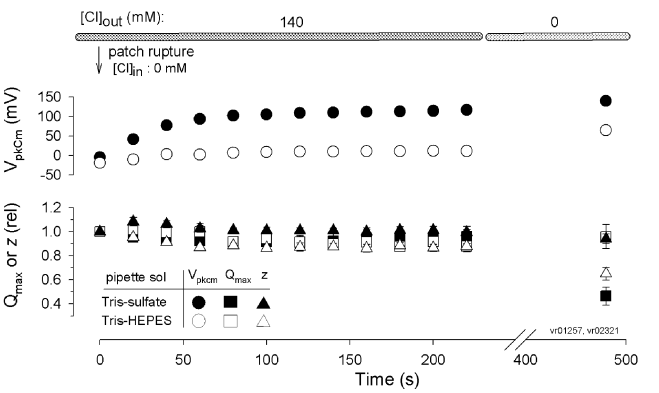

Figure 2. Boltzmann parameters of motor charge movement determined from capacitance functions during washout of intracellular Cl^-

Horizontal bar at top represents extracellular Cl^- concentrations ($[Cl]_{out}$) during whole-cell recording. Pipette contained either Tris-sulfate or Tris-Hepes solutions ($n = 5$ for each condition; mean ± S.E.M.). The dominant effect of Cl^- washout is a shift in V_{pkcm}, with small changes in Q_{max} and z. Error bars are within symbol dimensions for most data points. After removal of extracellular Cl^-, steady-state levels of parameters show changes that depend upon species of the intracellular substitute anion. Recordings began at the moment of patch rupture at a holding potential of 0 mV.

Our results differ from those of Oliver *et al.* (2001) since they found that non-linear capacitance was not affected by extracellular Cl^- manipulations and was abolished when intracellular Cl^- was removed. Figure 3*A* shows the relationship between extracellular Cl^- concentration and the magnitude of non-linear capacitance in OHCs. In this case, the extracellular Cl^- manipulations were made after the cells were allowed to equilibrate (> 5 min) with intracellular Tris-sulfate Cl^--free solutions. For comparison, Fig. 3*A* also shows the relationship between intracellular Cl^- concentration and Q_{max} (derived from non-linear capacitance) determined by Oliver *et al.* (2001). At concentrations above 5 mM, manipulation of Cl^- concentration on the extracellular aspect of the OHC membrane mirrored the effects obtained by Oliver *et al.* (2001) that relate to manipulation of intracellular Cl^-; however, we were unable to extinguish non-linear capacitance after total removal of extracellular (and intracellular) Cl^-. Another major difference between our results and theirs is our finding that very large shifts in V_{pkcm} occur not only as a function of intracellular- (see above) but also extracellular-Cl^- concentration (Fig. 3*B*). An increase in Cl^- concentration shifted V_{pkcm} to more negative potentials. The linear regression in Fig. 3*B* indicates a shift in V_{pkcm} of 0.37 mV mM^{-1} of extracellular Cl^- when Tris-sulfate Cl^--free intracellular solutions were used. In the presence of Tris-Hepes intracellular solutions, the shift was about 0.1 mV mM^{-1}. Thus, the magnitude of the shift was dependent upon the identity of the intracellular anion.

In order to determine if differences in intracellular control solutions were responsible for some of the discrepancies between our results and those of Oliver *et al.* (2001), we tested their major control anion, pentane sulfonate, and found that intracellular dialysis of such Cl^--free preparations (Table 1) had several atypical effects on OHC motor charge movement, compared with our other control anions. First, the initial peak C_m value (11.5 ± 1.1 pF; $n = 4$; collected within a few seconds after patch rupture) was about half that obtained with Tris-Hepes or Tris-sulfate solutions, indicating that the reduction following patch rupture was more rapid than the typical time course of ion washout (Pusch & Neher, 1988); the block is too fast to result from Cl^- removal during patch-pipette solution exchange. It is, however, typical of intracellular application of high affinity motor blockers, such as the charged form of salicylate, which blocks non-linear capacitance within seconds of patch rupture (Kakehata & Santos-Sacchi, 1996). As with salicylate, we still observed significant, though reduced, electromotility in all OHCs studied with

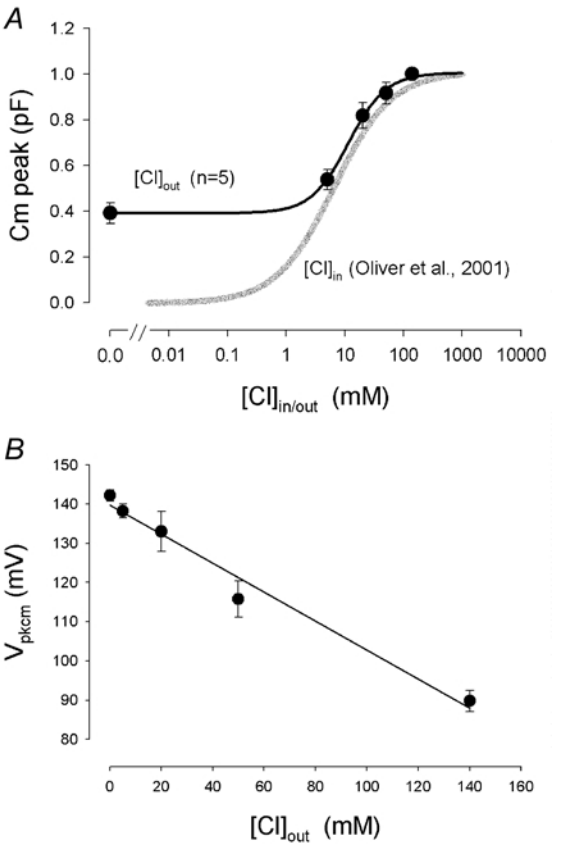

Figure 3. Dependence of peak C_m and V_{pkcm} on extracellular Cl^- concentration

A, continuous line is sigmoidal fit to data points (mean ± S.E.M.; $n = 5$). Intracellular solution was Tris-sulfate (Table 1) and initial extracellular solution was 140 Cl (Table 2). Extracellular Cl^- ($[Cl]_{out}$) reductions were made by replacement with Hepes. For comparison, we show relative Q_{max} (determined from capacitance measures) *vs.* intracellular Cl^- ($[Cl]_{in}$) concentration published by Oliver *et al.* (2001). *B*, same procedures as above. Line is linear regression ($r^2 = 0.98$) with a slope of 0.37 mV mM^{-1}.

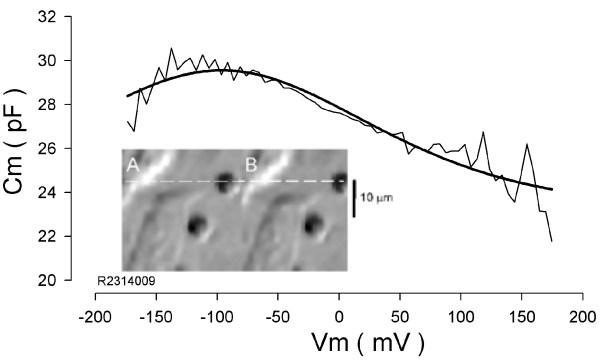

Figure 4. OHC non-linear capacitance and mechanical response with sodium pentane sulfonate patch-pipette solutions

In the presence of 140 Cl extracellular solution, and after steady-state intracellular perfusion of Cl^--free pentane sulfonate solution, non-linear capacitance remains significant, and mechanical responses during voltage stimulation are prominent. Smooth line is fit to eqn (1) (V_{pkcm}, −96 mV; z, 0.31; Q_{max}, 2.1 pC and C_{lin}, 23.2 pF, respectively. Inset: image of OHC at negative (*A*) and positive (*B*) extremes of voltage ramp. Note displacement of cuticular plate.

Table 1. Intracellular solutions

Solution name	Hepes (mM)	$Tris_2SO_4$ (mM)	Sodium pentane sulfonate (mM)	$MgSO_4$ (mM)	EGTA (mM)	Tris(OH) (mM), approx
Tris-Hepes	190	—	—	2	10	120
Tris-sulfate	10	110	—	2	10	35
Sodium pentane sulfonate	10	—	140	2	10	30

Cl^--free, pentane sulfonate solutions ($n = 5$; Fig. 4). At steady state (> 3 min), intracellular pentane sulfonate solutions decreased peak C_m to 78.1 ± 8.8 % of the initial value. Second, unlike the results with $Hepes^-$ or SO_4^{2-} intracellular anions, the subsequent removal of extracellular Cl^- had no effect on the substantial remaining non-linear capacitance (78.5 ± 4.6 % of initial value). Last, shifts in V_{pkcm} were in the hyperpolarizing direction during washout, as opposed to the other control anion solutions we used. Boltzmann fits of these data showed that voltage sensitivity (z) was substantially reduced, while total charge moved was minimally affected (sodium pentane sulfonate intracellular; Cl^--free Tris-Hepes extracellular: Q_{max}, 1.71 ± 0.20 pC; z, 0.33 ± 0.02; V_{pkcm}, −99 ± 12 mV; C_{lin}, 21.9 ± 0.7 pF; $n = 5$). These data clearly show that the effect of pentane sulfonate is not due to manipulation of intracellular Cl^-, but instead results from its direct action on the OHC motor.

Cl^- flux through a lateral membrane conductance influences prestin activity

Our data may indicate that in native, intact OHCs, extracellular Cl^- can influence the lateral membrane motor. Alternatively, Cl^- ions might be entering the OHC to work on the inner aspect of the lateral membrane. We evaluated this possibility by monitoring OHC currents and capacitance during whole-cell recording with Cl^--free intracellular solutions while manipulating extracellular Cl^- concentrations. Figure 5 shows results for a typical OHC held at 0 mV. As noted above, intracellular washout with Tris-Hepes solution causes an initial decrease in peak C_m, and a positive shift in V_{pkcm}, demonstrating the dependence of motor charge transfer on intracellular Cl^-. Subsequently, in the face of continuous intracellular washout, the removal of extracellular Cl^- betrayed an outward current (Cl^- influx) that sustained a substantial component of non-linear capacitance; in the absence of current, owing to the removal of extracellular Cl^-, capacitance again fell and V_{pkcm} shifted as intracellular Cl^- levels dropped. Steady-state levels were reached within minutes, which is typical for washout times under whole-cell voltage clamp (Pusch & Neher, 1988). Replenishment of extracellular Cl^- restored the Cl^- influx, thereby increasing the non-linear capacitance of the cell and shifting V_{pkcm} back to hyperpolarized levels. These effects were repeatable. These experiments demonstrate that in the absence of Cl^- in the patch pipette, the source of intracellular Cl^- that modulates prestin derives from the extracellular solution.

In order to localize the Cl^- conductance, we directly mapped the increase in non-linear capacitance and Cl^- current as a restricted source of Cl^- roved along the length of OHCs whose intracellular Cl^- was depleted (Fig. 6). The largest responses were obtained along the lateral region of the OHC, in the same region where prestin is localised (Belyantseva *et al.* 2000*a*), and the reciprocal electro–mechanical sensitivity of the motor is found (Takahashi & Santos-Sacchi, 2001). Further confirmation of this conductance site is provided by reversal potential measurements during application of extracellular Cl^- solutions (see supporting data below). The site of this Cl^- conductance is ideally poised to affect the activity of prestin rapidly.

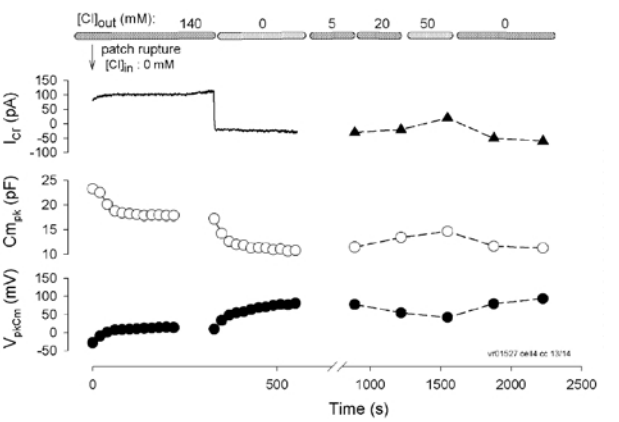

Figure 5. Correspondence among Cl^- current, peak non-linear C_m and V_{pkcm}

Horizontal bars at top represent extracellular Cl^- concentrations ($[Cl]_{out}$) during whole-cell recording. Recordings began at the moment of patch rupture with Tris-Hepes Cl^--free pipette solution at a holding potential of 0 mV. Despite a large sustained inward Cl^- flux (outward current; I_{Cl}, top), non-linear C_{mpk} decreases (middle), and V_{pkcm} shifts to depolarized levels (bottom) during Cl^- washout through the patch pipette. Subsequent removal of extracellular Cl^- shifts C_{mpk} and V_{pkcm} values further, showing their dependence on Cl^- influx into the cell. The treatments are reversible and responses are graded with magnitude of Cl^- current. ($[Cl]_{in}$), intracellular $[Cl^-]$.

Table 2. Extracellular solutions

Solution name	Hepes (mM)	HCl (mM)	NaOH (mM)	KOH (mM)	Tris(OH) (mM), approx	$MgSO_4$ (mM)	$CaSO_4$ (mM)
Tris-Hepes	210	—	—	—	110	5	0.2
140 Cl	10	140	—	—	155	5	0.2
80 Cl	108	80	—	—	30	5	0.2
80 Na	220	—	80	—	—	5	0.2
80 K	220	—	—	80	—	5	0.2

Cl^- channels do not underlie the lateral membrane conductance

Guinea-pig OHCs typically have a relatively low membrane resistance (< 300 MΩ) even in the presence of K^+ and Ca^{2+} channel blockers (Santos-Sacchi, 1991*b*; Santos-Sacchi & Navarrete, 2002). However, when OHCs were perfused with solutions containing mainly large, poorly permeable ions (Tris-Hepes, see Tables 1 and 2), input resistances ranged from 1–3 GΩ. Under these conditions, with approximately equal amounts of $Tris^+$ and $Hepes^-$ as major charge carriers intra- and extracellularly, whole-cell steady-state currents revealed non-linear current-to-voltage characteristics (*I–V*s) reversing near 0 mV ($V_{rev,TH}$ = +1 ± 1 mV, range: −3 to +6 mV, n = 20); moderate inward and outward rectification was evident at hyperpolarizing and depolarizing potentials (Fig. 7*Aa,b* and *B*). The activation phase of currents at any voltage was faster than our clamp-time constant, typically less than 1 ms. These control currents were not influenced by the stereocilia transducer channel blocker streptomycin (500 μM) and were not due to an imperfect seal between patch pipette and OHC membrane, since their *I–V*s showed clearly reproducible non-linear, sigmoidal shapes. Preconditioning hyperpolarizing steps did not influence the current at +60 mV (Fig. 7*Aa* and *B*). Additionally, a pre-depolarizing step to +60 mV did not influence the subsequently evoked currents at a variety of membrane potentials (Fig. 7 *Ab* and *B*), indicating that no slow-type inactivation of these currents (5 ms < τ < ~100 ms) exists at any physiological membrane potential.

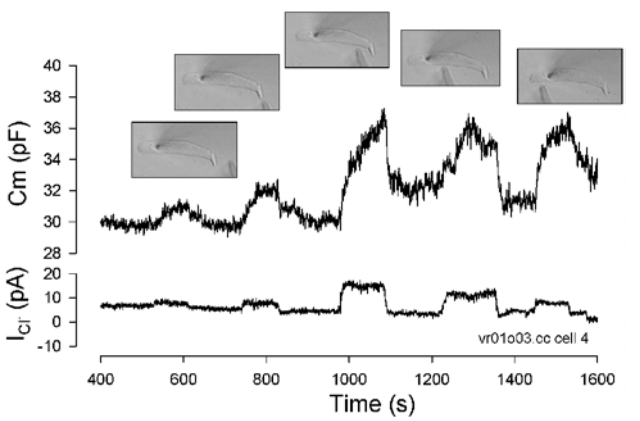

Figure 6. Localization of the Cl^- conductance to the lateral membrane

A 1 M Cl^- point-diffusion source (high impedance pipette), briefly positioned close to different OHC regions (image insets), revealed a maximum increase in I_{Cl} and C_m in the mid region of the cell. After each placement, the pipette was moved away from the cell and is indicated as a return of current and capacitance to near baseline.

To study the Cl^- permeability of the conductance responsible for the sigmoidal currents observed in Tris-Hepes solutions, we substituted the bulk of extracellular Hepes with 140 mM TrisCl. This substitution significantly and reversibly increased both inward and outward currents, whose kinetics, absence of slow gating and sigmoidal shape of *I–V*s were the same as for Tris-Hepes currents (Fig. 7*Ac,d* and *B*). The reversal potentials in 140 mM TrisCl extracellular solution ($V_{rev,140Cl}$) were smaller in magnitude than expected, but appropriate in polarity ($V_{rev,140Cl}$ = −12 ± 2 mV, range: −33 to −1 mM; n = 20). This deviation presumably derives from rapid equilibration of ions into the restricted space (~33 nm) between the lateral plasma membrane and subsurface cisternae (Pollice & Brownell, 1993). It is well known that such ion accumulation under whole-cell voltage clamp can affect reversal potentials and provide apparent changes in ion selectivity (Frazier *et al.* 2000). Accordingly, then, Cl^- applied extracellularly was the major carrier for outward currents (Cl^- influx), and its intracellular accumulation provided for the inward current component (Cl^- efflux).

In addition to Cl^-, we tested whether the major monovalent cations, K^+ and Na^+, could carry measurable currents through this lateral membrane conductance. In the same cells, 80 mM K^+, Na^+ and Cl^- were sequentially substituted in the external solution for the equivalent amount of poorly permeable ions (K^+ and Na^+ for $Tris^+$, Cl^- for $Hepes^-$). In these experiments, 1 mM 4AP and 200 μM linopirdine were added to all solutions to block voltage-dependent potassium channels described earlier in OHCs (Santos-Sacchi & Dilger, 1988; Marcotti & Kros, 1999). All three substitutions increased both inward and outward components of the currents above controls (Fig. 7*C*). In fact, the resulting currents showed kinetics and rectification resembling those observed in reference Tris-Hepes solutions (Fig. 7*C* and *E*).

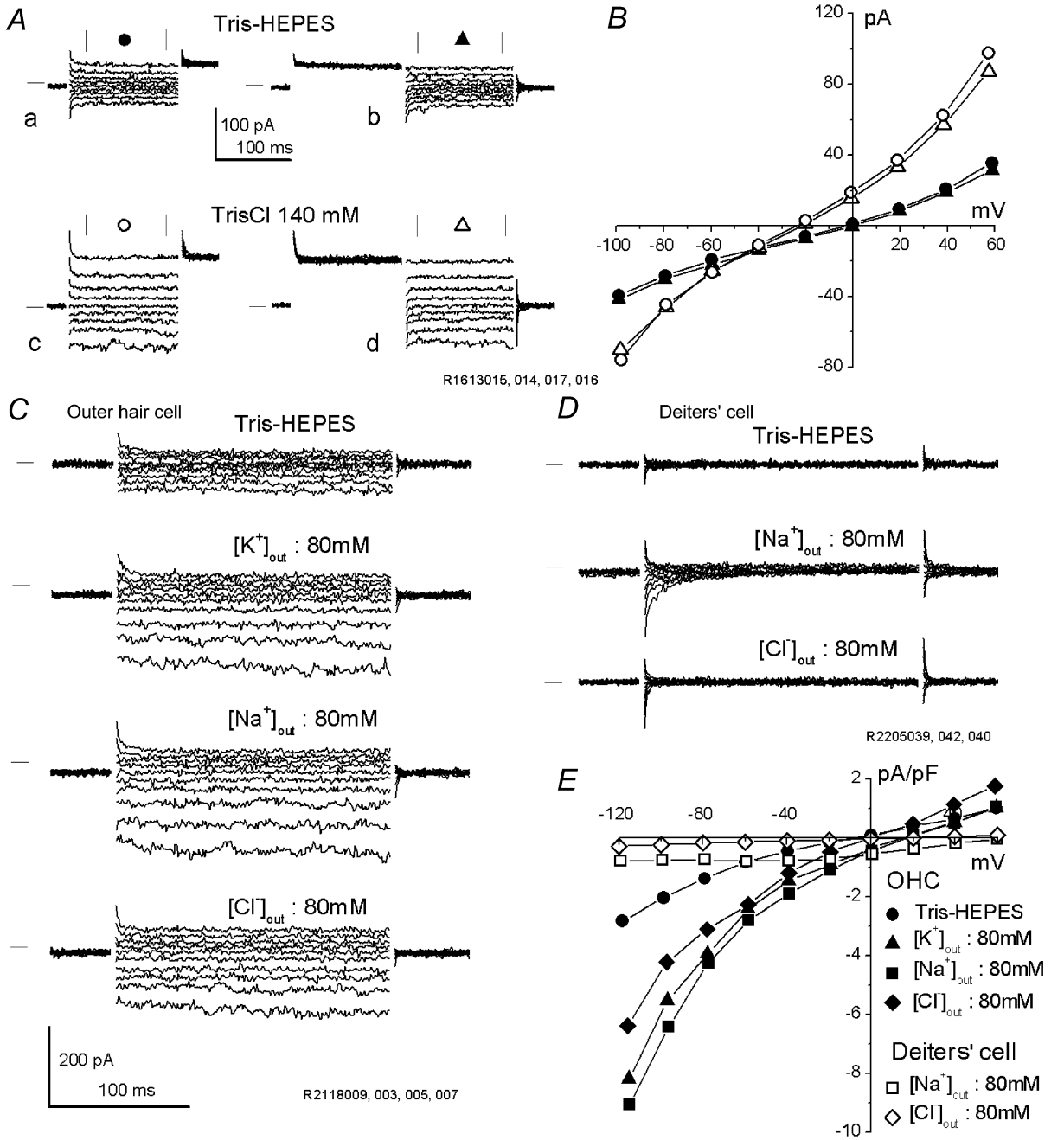

Figure 7. OHCs possess a voltage-dependent, cation–anion non-selective conductance

All recordings were made with Tris-Hepes intracellular solution (Table 1). *A*, currents recorded in the same OHC subjected to voltage pre-conditioning step protocol (*a*,*c*: holding potential, $V_{hold} = -20$ mV, 150 ms conditioning steps from −100 to +60 mV ($\Delta V = 20$ mV), 150 ms test step to +60 mV) and pre-depolarizing step protocol (*b*,*d*: $V_{hold} = -20$ mV, 150 ms conditioning step to +60 mV, 150 ms test steps from −100 to +60 mV ($\Delta V = 20$ mV)) in Tris-Hepes reference extracellular solution (*a*, *b*) or 140 mM TrisCl-based (140 Cl) extracellular solution (*c*, *d*). Horizontal lines at left of traces indicate zero-current level. *B*, series-resistance corrected *I*–*V* curves from currents in *A*, trace averaged between vertical marks. *C*, OHC currents recorded in (top to bottom) Tris-Hepes, 80 K, 80 Na and 80 Cl extracellular solutions (Table 2) in the presence of 1 mM 4AP + 200 μM linopirdine, evoked by voltage steps from +60 to −120 mV ($\Delta V = -20$ mV) from $V_{hold} = -20$ mV. Records are from the same OHC. *D*, Deiters' cell currents recorded in (top to bottom) Tris-Hepes, 80 Na and 80 Cl extracellular solutions, evoked by the same voltage protocol as in *C*. Scale is same as in *C*. *E*, relative currents for OHC and Deiters' cell from *C* and *D* above, normalized by their membrane capacitance (24.7 pF linear capacitance for OHC and 21.8 pF linear capacitance for Deiters' cell).

In order to study further the accumulation of ions into the restricted sub-plasmalemmal space, we compared the reversal potentials of currents obtained in 80 mM $[Na^+]_{out}$- and 80 mM $[Cl^-]_{out}$-containing extracellular solutions and found that although they were appropriate in polarity, they were smaller in magnitude than expected ($V_{rev,80Na}$ = +29 ± 2 mV, range: 17 to 39 mV, n = 12; $V_{rev,80Cl}$ = −16 ± 3 mV, range: −33 to +3 mV, n = 14). These results clearly indicate that both extracellular cations and anions can accumulate in the sub-plasmalemmal space of the OHC at our holding potential of 0 mV. For Cl^-, the Nernst equation shows that an intracellular concentration of ~40 mM was achieved at steady state with 80 mM Cl^- extracellularly. The same calculations for Na^+ show an intracellular concentration of ~30 mM. No indication of a similar conductance was found under the same experimental conditions in isolated supporting Deiters' cells, which lack prestin but have approximately the same size and passive membrane capacitance as OHCs (Fig. 7*D* and *E*). Normalized conductance of Deiters' cells in Tris-Hepes and 80 mM $[Cl^-]_{out}$ (80 Cl) extracellular solutions was (n = 5) 1.0 ± 0.05 and 2.28 ± 0.73 pS pF^{-1}, respectively. For comparison, OHC conductance was 15.6 ± 5.5 and 56.6 ± 18.9 pS pF^{-1}, respectively.

We found that steady-state Cl^- current levels remain stable for several seconds at membrane potentials from −80 to +40 mV (Fig. 8*A*). However, during prolonged hyperpolarizations more negative to −100 mV, a slowly developing increase in current was often observed. Because such behaviour might be characteristic of ClC-2 chloride channels,

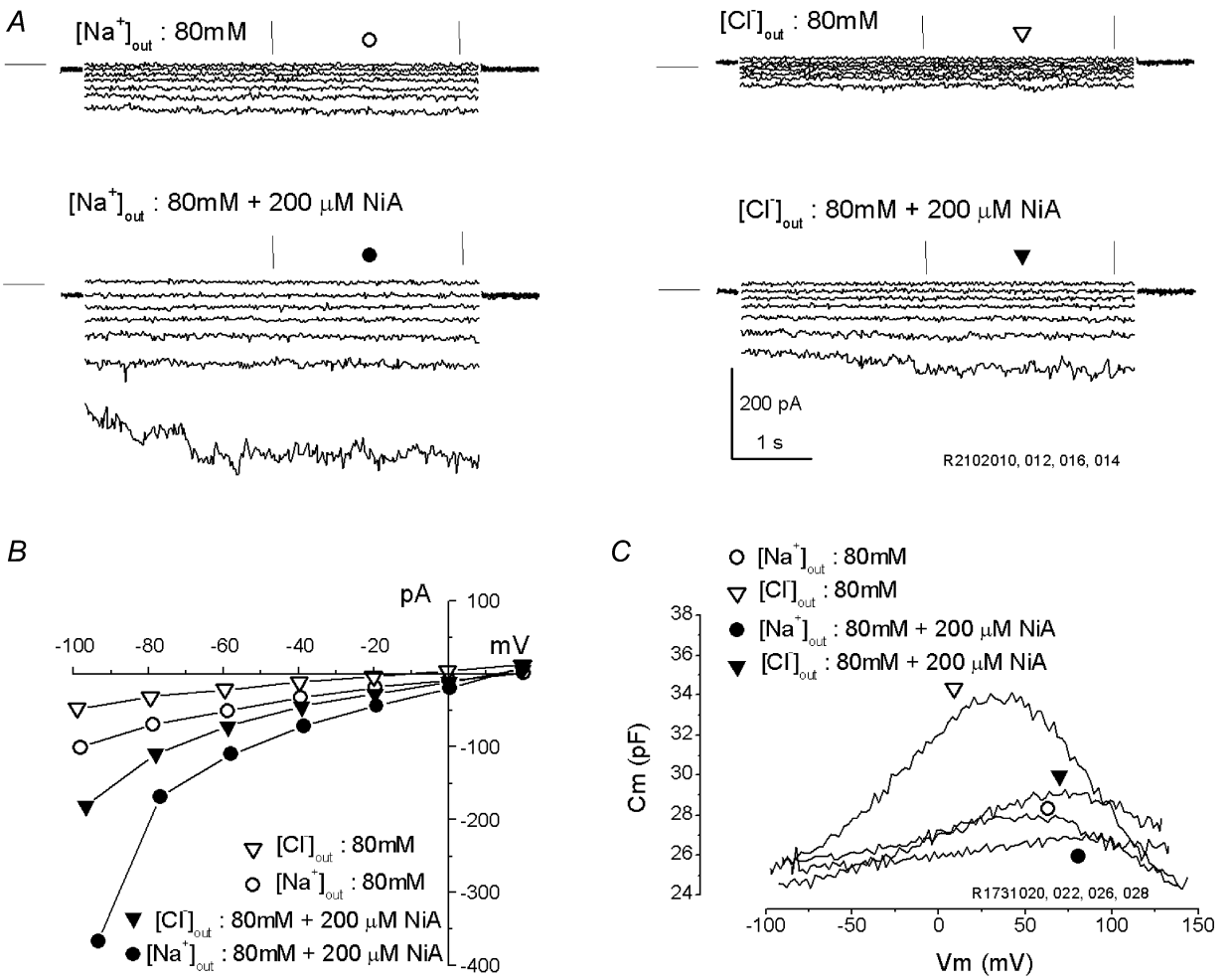

Figure 8. Cl^- channel blockers increase the lateral membrane conductance but block non-linear capacitance

A, currents were evoked by prolonged (5 s) pulses from +20 to −100 mV (step = −20 mV) from V_{hold} = 0 mV. Data were collected from the same OHC in 80 Na (left) or 80 Cl (right) extracellular solutions (Table 2), in the absence (top) or in the presence (bottom) of 200 μM niflumic acid (NiA). Horizontal lines at left of traces indicate zero-current level. Note the identical kinetics, voltage dependence and increase by NiA for Na^+ and Cl^- currents. *B*, *I–V* plots obtained from trace averages (between vertical marks) in *A* above. *C*, *C–V* functions obtained from another OHC after treatments as in *A* above. Note potent block of niflumic acid of prestin-related non-linear capacitance, despite enhanced inward–outward Cl^- currents.

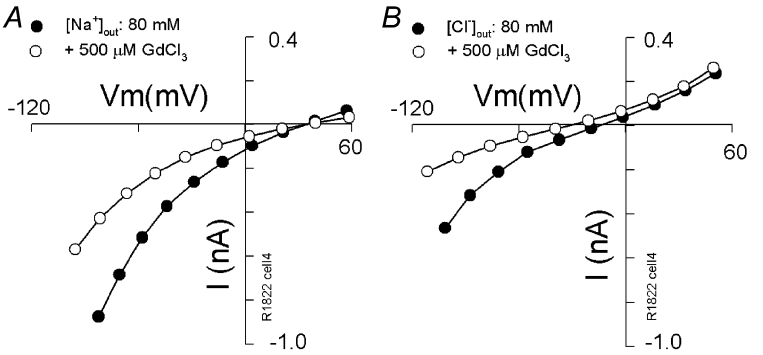

Figure 9. Partial block of the lateral membrane conductance by gadolinium

OHC *I–V* plots with extracellular solutions 80 Na (*A*) or 80 Cl (*B*) without (●) and with (○) the stretch-channel blocker gadolinium (500 μM) obtained in the same cell.

we compared the currents at long hyperpolarizing potentials in 80 mM $[Na^+]_{out}$ and 80 mM $[Cl^-]_{out}$ extracellular solutions. Cl^- channels are not expected to pass cations. In either solution the slowly developing component was observed. Additionally, well-known Cl^- channel blockers (niflumic acid 200–400 μM, DIDS 0.5–2.5 mM, furosemide 200 μM, NPPB 10–500 μM, 9-AC 1–2 mM; (Jentsch *et al.* 2002)) did not decrease the currents. Instead, $Cl^-$and Na^+ currents, including the slow component, were reversibly increased. For example, niflumic acid at 200 μM increased the Cl^- current by a factor of 3.4 at −75 mV, while the Na^+ current was increased by a factor of 2.2 ($n = 3$). Figure 8*B* and *C* illustrates the effect of niflumic acid (200 μM) on currents and capacitance. While currents were increased, non-linear capacitance was reduced; in fact, niflumic acid was a potent blocker of non-linear capacitance, working in the micromolar range. Additionally, a slowly developing outward component, never observed in ClC-type channels, could also be observed at large depolarizing potentials (more positive to +60 mV), but could not be studied in detail because of irreversible damage to the OHC at prolonged depolarizations. Taken together, these observations clearly indicate that ClC channels, whose messenger RNA is found in OHCs (Kawasaki *et al.* 1999), or other clearly characterized types of Cl^- pathways (cystic fibrosis trans-membrane conductance regulator (CFTR), transporters), do not underlie the non-selective conductance of the lateral membrane.

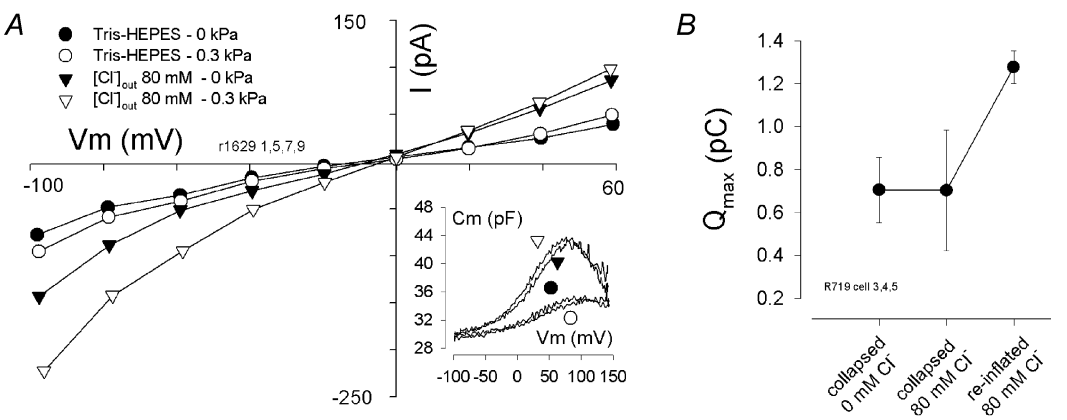

Figure 10. Membrane tension dependence of the Cl^- current

A, sigmoidal *I–V* curves were derived from trace-averaged currents recorded with Cl^--free Tris-Hepes patch pipette in the presence of Tris-Hepes (circles) and 80 Cl (triangles) extracellular solutions before (filled symbols) and after (open symbols) turgor pressure increases in the initially cylindrical OHC ($V_{hold} = 0$ mV, step from +60 to −100 mV). Currents are substantially increased and pressure sensitive in Cl^--containing solution. Inset: *C–V* functions, corresponding to the treatments in *A*, reflect a significant increase in membrane displacement charge and are shifted in the hyperpolarizing direction in Cl^--containing solution. The additional charge increase and C_m shift in the pressurized state (▽) is due to increased Cl^- flux, because in Cl^--free solutions (○), as well as in Cl^--saturated solutions (Kakehata & Santos-Sacchi, 1995), the C_m functions are shifted to depolarizing potentials with positive pressure. *B*, non-linear charge (Q_{max}), determined from *C–V* function fits ($n = 3$) does not increase in initially collapsed cells in Cl^--containing extracellular solution (140 Cl) until Cl^- flux is restored by cell re-inflation.

The lateral membrane current is partly reduced by blockers of stretch-activated conductances

Thus far we have ruled out the contribution of Cl^- and stereocilia transducer channels to the conductance we observe. In addition, we have evaluated other blockers of channels that conceivably could support components of the lateral membrane current. Blockers of aquaporin ($HgCl_2$ 0.4–2 mM; (Belyantseva *et al.* 2000*b*)), gap junction hemichannels (carbenoxolone 200 μM, octanol 2 mM; (Santos-Sacchi, 1991*a*; Draguhn *et al.* 1998)) and cation-selective vanilloid receptor channels (Ruthenium Red; (Gunthorpe *et al.* 2002)) were without success. Additionally, the absence or presence of intra/extracellular Ca^{2+}, or the presence of intracellular ATP and GTP did not affect the currents.

Finally, we evaluated agents known to block swelling-activated conductances. Stretch-activated channels have been found in the lateral membrane of OHCs; however, they are selective for cations (Ding *et al.* 1991; Iwasa *et al.* 1991). Several blockers were partly effective. Gadolinium (Gd^{3+}; 500 μM, $n = 5$; Fig. 9), tamoxifen (50 μM, $n = 4$–7) and quinine (1 mM, $n = 4$) were from 10 to 40 % effective at −60 mV in blocking Na^+ (relative I, Gd^{3+}: 0.59 ± 0.07, quinine: 0.74 ± 0.05, tamoxifen: 0.77 ± 0.04) and Cl^- currents (Gd^{3+}: 0.72 ± 0.2, quinine: 0.76 ± 0.16, tamoxifen: 0.91 ± 0.16). Whereas Gd^{3+} effectively blocked OHC capacitance and motility, even in the presence of high Cl^- levels (Santos-Sacchi, 1991*b*), tamoxifen and quinine did not. These blockers are non-specific, inasmuch as they have been shown to block a variety of anionic and cationic channels, some involved in cell swelling (Yang & Sachs, 1989; Allen *et al.* 1998; Welsh *et al.* 2000). Interestingly, tamoxifen and quinine are known to block swelling of OHCs in cochlear explants (Siegel *et al.* 2001), and Gd^{3+} interferes with volume regulation in isolated OHCs (Crist *et al.* 1993).

One other agent, poly-lysine (4 μM, molecular weight 70 000–150 000), which has been shown to block stretch-induced mechanical responses in OHCs (Brundin *et al.* 1989), had a small blocking effect on both Na^+ (relative I: 0.90 ± 0.2; $n = 3$) and Cl^- (relative I: 0.84 ± 0.13; $n = 3$) currents at −60 mV. Poly-lysine, which might be considered a potent charge-screening agent, had virtually no effect on the reversal potentials of the currents.

The Cl^- conductance is stretch sensitive and gated at acoustic rates

Since the lateral membrane ionic current was susceptible to stretch-activated channel blockers, we evaluated its response to membrane stress with a variety of means

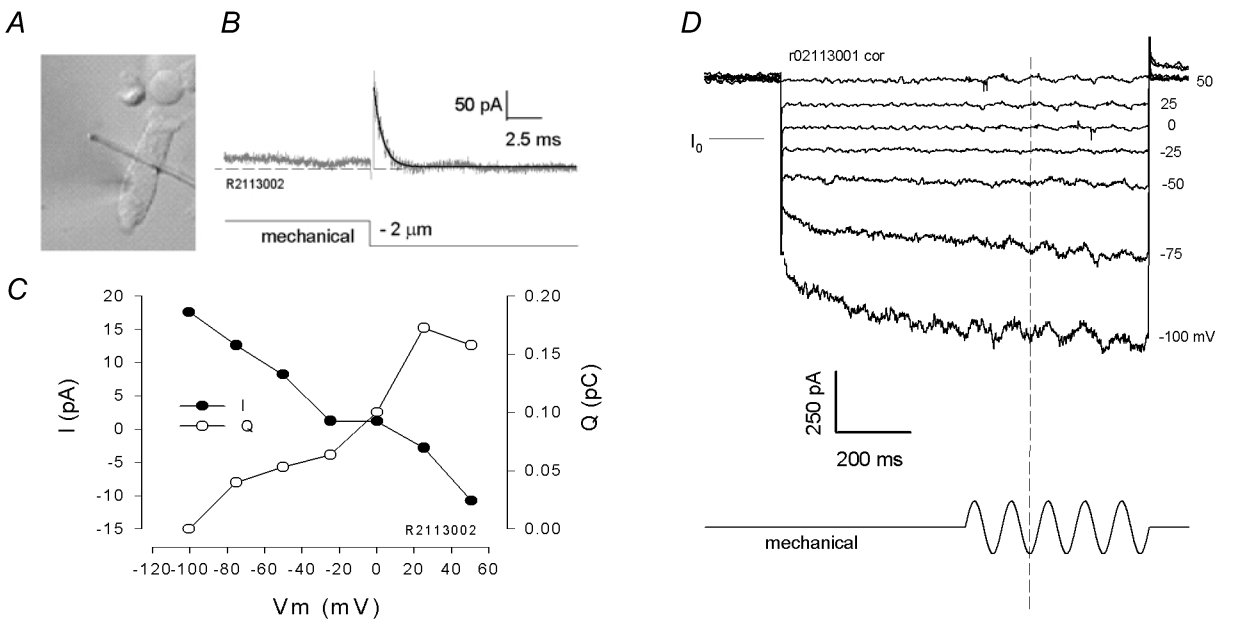

Figure 11. Whole-cell current responses evoked by stiff probe deformations of the lateral membrane

A, digitally captured image of OHC under whole-cell voltage clamp with stiff probe placed across the middle of the cell. *B*, step mechanical deformation of the lateral membrane evokes a transient gating current and a DC ionic current at the fixed potential of 50 mV. *C*, relationship of motor gating charge (integrated transient current, Q) and ionic current magnitude (I, difference between steady-state levels before and after membrane stress) with membrane voltage. Motor charge peaks at V_{pkcm}, whereas I reverses at the potential (−10.5 mV) where total current reverses. *D*, sinusoidal mechanical stimulation at various potentials produces a corresponding current whose phase reverses at the cell's steady ionic current reversal potential. Extracellular solution was 140 Cl and intracellular was Tris-Hepes + 1 mM Tris-Cl^-.

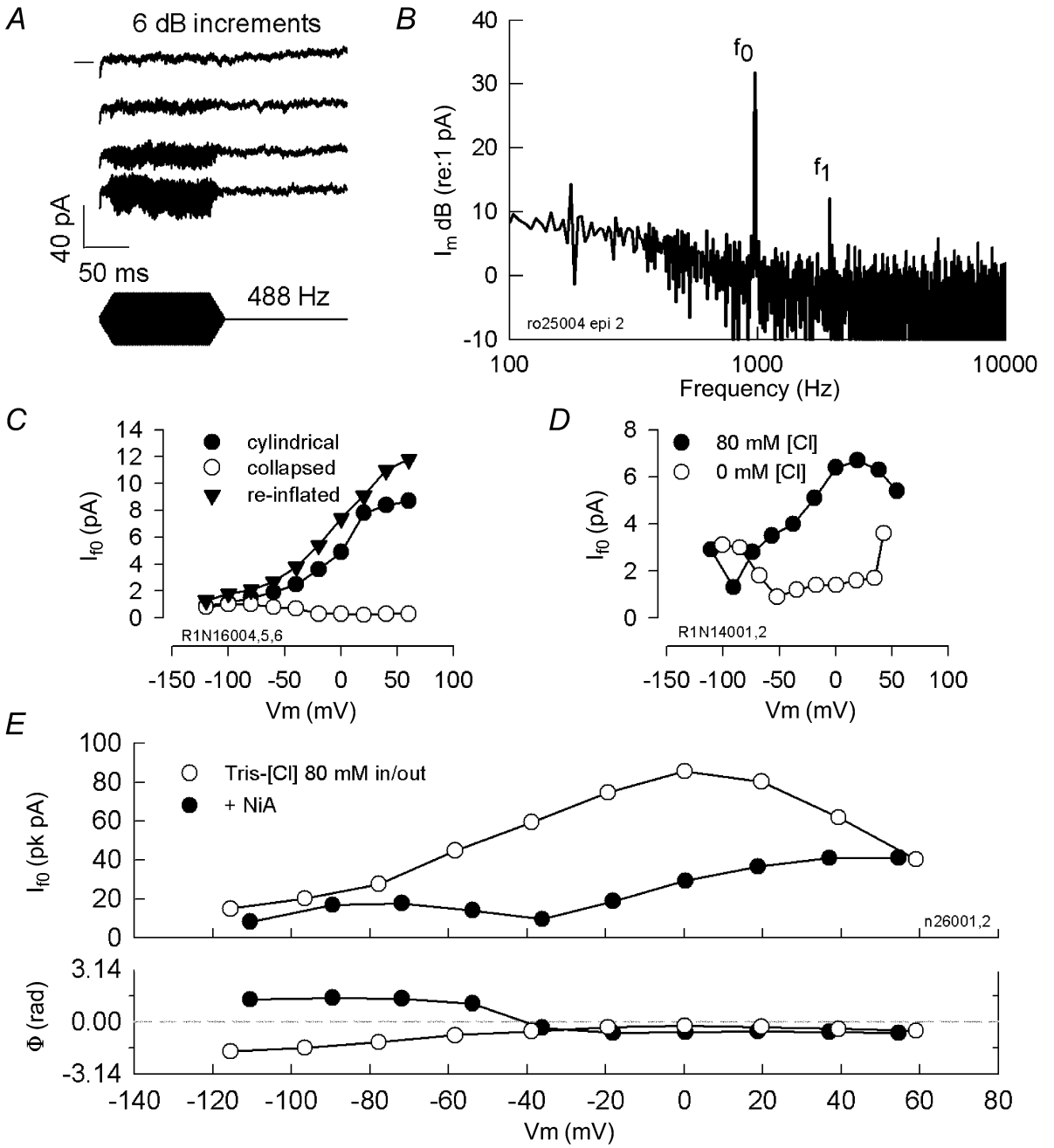

Figure 12. Whole-cell current responses evoked by fluid-jet stimulation of the lateral membrane

A, traces depict an intensity series (6 dB increments in the voltage that drives the piezoelectric fluid-jet) at 488 Hz. Note AC and DC components. DC components grow with stimulus level indicating that they do not arise from bottoming out of the piezoelectric driver. Zero current level is indicated by horizontal line on left of top trace. Traces are separated vertically for clarity. Tris-Hepes intracellular *vs.* 80 Cl extracellular. *B*, fundamental (f_0) and first harmonic (f_1) are present in FFT transform from whole-cell currents generated by OHC in response to 1 kHz fluid-jet mechanical stimulation against the lateral wall of the cell. I_m, membrane current plotted on a decibel scale. *C*, I_{f0} is blocked by collapsing the OHC with negative pipette pressure; re-inflation restores the current. Niflumic acid (250 μM)-treated OHC. *D*, removal of extracellular Cl^-, in the absence of intracellular Cl^- reduces the fluid-jet evoked current. *E*, the reduction of non-linear peak capacitance after 250 μM niflumic acid (NiA) treatment (16.6 pF (V_{pkcm}: −12.7 mV) *vs.* 8.63 pF (V_{pkcm}: 20.3 mV) derived from *C*–*V* functions) produced a reduction of the capacitive component and shift in the current's voltage dependence to the depolarized levels. Consequently, characteristics of the ionic component are revealed as I_{f0} magnitude displays a minimum where an abrupt phase reversal occurs. Tris-Hepes-based intracellular solution (10 mM [Cl^-]); extracellular solution 80 Cl.

including turgor pressure modulation, and localized membrane deformation with stiff probe and fluid jet. In the presence of only poorly permeable ions inside and outside the OHC, increasing intracellular pressure had only a slight effect on the resting conductance of the cell; subsequent to the addition of extracellular Cl^- the effect was much more pronounced (Fig. 10*A*). For example, at −60 mV the Cl^- current was nearly doubled. Simultaneous with the increase in Cl^- flux, the non-linear capacitance was augmented. In this example, the OHC was cylindrically shaped throughout the experiment, that is, there was tension on the membrane even when no positive pipette pressure was administered (0 kPa). The effect of the stretch sensitivity of the current on non-linear capacitance was more clearly appreciated when re-inflating initially collapsed OHCs, where the initial tension on the lateral membrane was minimal or absent (Fig. 10*B*). Indeed, the augmentation of non-linear capacitance or charge movement by restoring extracellular Cl^- did not occur in OHCs that had been collapsed with negative pressure prior to the restoration, but ensued when the cells were returned to a cylindrical shape by positive intracellular pressure. The resulting increase in membrane tension caused an influx of Cl^- ions, and an augmentation of prestin-generated charge movement.

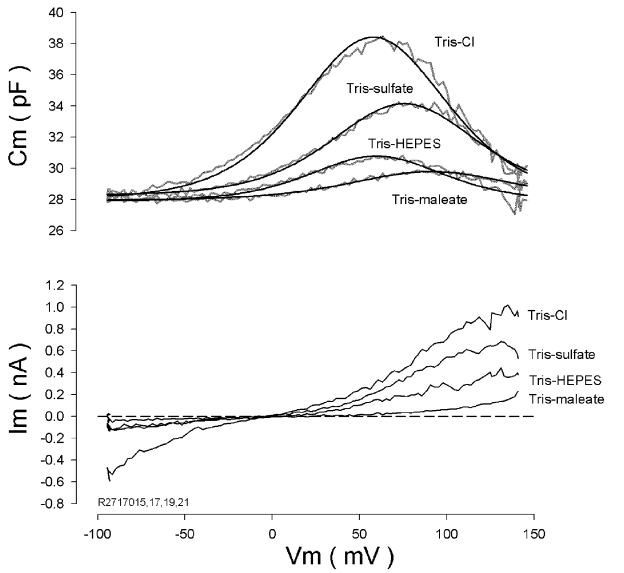

Figure 13. Effects of control anions on OHC non-linear capacitance and current

A, the OHC was perfused with solutions of minimal composition in order to evaluate the effects of control anions. The intracellular solution was maleate-based (mM: 120 maleate, 250 Tris, 2 EGTA). The initial extracellular maleate-based solution (mM: 120 maleate, 250 Tris) was sequentially substituted by Tris-Hepes (mM: 220 Hepes, 60 Tris), Tris-sulfate (mM: 120 SO_4^{2-}, 250 Tris) and Tris-Cl (mM: 155 Cl^-, 165 Tris) solutions. Capacitance measures and corresponding fits (smooth lines) to eqn (1) provide Boltzmann parameters for the tested anions: (maleate: V_{pkcm}, 91 mV; z, 0.82; Q_{max}, 0.23 pC; C_{lin}, 27.96 pF; Hepes: V_{pkcm}, 60 mV; z, 0.99; Q_{max}, 0.30 pC; C_{lin}, 27.89 pF; sulfate: V_{pkcm}, 75 mV; z, 0.92; Q_{max}, 0.65 pC; C_{lin}, 28.28 pF; Cl^-: V_{pkcm}, 58 mV; z, 0.91; Q_{max}, 1.16 pC; C_{lin}, 28.0 pF. *B*, corresponding ionic currents generated by downward voltage ramps (+150 to −100 mV, 125 ms; corrected for ramp-induced passive capacitive offset current component – 52 pA for this cell). Note increasing outward (inward anionic) currents associated with the different anions, and the corresponding increases in non-linear capacitance.

The stretch sensitivity of the Cl^- current was further tested by mechanically stimulating the lateral membrane with stiff glass probes (Fig. 11*A*). A step change in membrane deformation evoked an initial transient current due to motor charge movement, followed by a shift in steady-state current (Fig. 11*B*). As expected, the magnitude of the charge moved was dependent on holding potential and reached a maximum at positive potentials where V_{pkcm} resides under these ionic conditions (Gale & Ashmore, 1994; Zhao & Santos-Sacchi, 1999) (Fig. 11*C*). On the other hand, the polarity of the mechanically induced component of the ionic current reversed near the reversal potential (−10.5 mV) of the total ionic current. Low frequency AC stimulation with the probe generated corresponding AC currents whose phase reversed at the reversal potential of the current. The reversals in total current polarity are not exactly 180 deg since only a pure ionic current is expected to show this behaviour. These data are consistent with a dual-component current, one capacitive (motor-based) and one ionic.

Finally, in order to assess the physiological significance of the conductance better, we studied its gating by deformation of the lateral membrane at acoustic rates. We used stimulus frequencies that were physiologically appropriate for the OHCs that we isolated, namely for cells whose characteristic frequency ranged up to about 1 kHz (Dallos *et al.* 1982). Figure 12 illustrates that mechanical perturbation of the lateral membrane with micropipette-based, fluid-jet stimulation delivered at frequencies up to 1 kHz. The mechanical perturbation generated high frequency whole-cell currents that display distortion, including harmonic (I_{f1}) and DC components (Fig. 12*A* and *B*). This type of stimulation had been used previously to generate, poly-lysine-sensitive, tuned AC and DC mechanical responses from isolated OHCs (Brundin *et al.* 1989; Brundin & Russell, 1994); however, we did not measure the mechanical response of the cell under these conditions, which in any case would not be readily observable with our video sampling rate . We found strong evidence that the evoked current results from direct mechanical perturbation of the lateral cell membrane and is Cl^- dependent. First, it was generated only in OHCs possessing positive turgor pressure, and was reversibly abolished when the cells were collapsed (Fig. 12*C*). This dependence is similar to that of the mechanical sensitivity of prestin in the lateral membrane (Takahashi & Santos-Sacchi, 2001). Second, in the absence of intracellular Cl^-,

removal of extracellular Cl^- abolished or reduced the current (Fig. 12*D*).

Since it is known that mechanical stimulation of the lateral membrane can generate non-linear capacitive currents (Gale & Ashmore, 1994; Zhao & Santos-Sacchi, 1999; Takahashi & Santos-Sacchi, 2001), we performed experiments to dissociate capacitive and ionic components of the high frequency current. As with our stiff probe experiments, several pieces of evidence indicate that it is composed of capacitive as well as ionic components. First, while DC current components (Fig. 12*A*) are not expected for mechanically driven capacitive currents, they can arise from the rectified ionic conductance we described above. Second, in cells that were treated with niflumic acid to decrease non-linear capacitance and increase ionic (Cl^-) currents, I_{f0} showed two maxima: one near V_{pkcm}, where the non-linear capacitive component is largest (Gale & Ashmore, 1994; Zhao & Santos-Sacchi, 1999), and another at hyperpolarized potentials, where the ionic component is largest (Fig. 12*E*). Third, magnitude minima corresponded to abrupt phase changes, as expected for an ionic, but not for a mechanically driven capacitive current. The phase change in current polarity is not exactly 180 deg since only a purely ionic current is expected to show this behaviour. Based on results from all three methods of mechanical stimulation, we conclude that the mechanically evoked currents arise from two sources – the ionic conductance we described above, and the intrinsic displacement currents of the voltage sensor of prestin.

A role for sulfonic moieties in prestin activation

Since our observations and those of Oliver *et al.* (2001) suggest that variations in the cationic composition of solutions do not produce substantial effects on the non-linear capacitance of prestin, it is possible that our major control anions, $Hepes^-$ and SO_4^{2-}, could play a role as co-factors supporting the charge translocation of prestin. The common structural feature between these two anions is the presence of a negatively charged sulfonic group, SO_3. To explore the possible active role of sulfonate-containing molecules in prestin functioning further, we performed one last set of experiments using maleate (divalent, sulfonic-free) as control anion, in place of $Hepes^-$ and SO_4^{2-} (Fig. 13). Under symmetrical maleate solutions intra- and extracellularly, a small non-linear capacitance still remained. However, the exchange of extracellular solutions with Tris-Hepes, Tris-sulfate, or Tris-Cl produced an increase in non-linear capacitance and a further shift in V_{pkcm}. Thus, each of these anions is able to permeate the lateral membrane through the non-selective conductance we describe above, and activate prestin. We conclude that in the intact OHC, maleate, which lacks a sulfonic group, is barely active, while $Hepes^-$ and SO_4^{2-}, which possess sulfonic groups, partially support prestin activity similar to Cl^-.

DISCUSSION

We report several new observations. (1) Motor charge movement remains substantial in the absence of Cl^- and other known active anions inside and outside the intact OHC. (2) Cl^- ions significantly affect the state probability of prestin. (3) A Cl^- current through a non-selective lateral membrane conductance modulates prestin activity thereby making the OHC responsive to extracellular Cl^-, and (4) the Cl^- current is stretch sensitive and gated at acoustic rates. Taken together, these observations have substantial impact on our understanding of OHC function.

How does Cl^- work on prestin?

The current state. Recently, Oliver *et al.* (2001) proposed that prestin possesses an extrinsic voltage sensor where charge movement arises due to the binding and subsequent translocation of Cl^- or other anions from the intracellular to the extracellular aspect of the plasma membrane of the cell; simultaneous with this translocation, prestin is driven to the expanded state producing cell elongation. Intracellular SO_4^{2-} ions were ineffective in promoting charge movement, as were extracellular Cl^- ions. This was observed in native OHC membrane patches and whole-cell recorded prestin-transfected CHO cells.

Evidence for a new state. One of the main differences that we have with the the data of Oliver *et al.* (2001) is our observation of large shifts in the operating voltage of the motor (V_{pkcm}) during intracellular Cl^- removal. Since we first presented evidence for this phenomenon (Rybalchenko & Santos-Sacchi, 2001), we realized that the simple voltage sensor scheme of Oliver *et al.* (2001) was incomplete. A shift in V_{pkcm} suggests significant changes in the energy profile for voltage-dependent motor transitions regardless of whether extrinsic or intrinsic voltage sensors control prestin. Supporting this contention, we previously showed that salicylate, working on the inner aspect of the lateral plasma membrane, not only reduces the voltage sensitivity of the motor (z), but shifts V_{pkcm} in the positive direction (Kakehata & Santos-Sacchi, 1996), indicating a more complex interaction than simple competition for an extrinsic sensor's binding site as suggested by Oliver *et al.* (2001).

Another major difference between our data and that of Oliver *et al.* (2001) is that we find that extracellular Cl^- can enter the cell through a lateral membrane stretch-activated conductance to influence prestin activity. Since they studied excised membrane patches, it is possible that in the absence of applied tension to the patch, the conductance was inactive. Additionally, in transfected cells the conductance may not have been expressed. In their motility studies on intact OHCs, the use of intracellular pentane sulfonate solutions confounded the evaluation of Cl^- effects.

Finally, the most controversial difference between our data and theirs is our observation that SO_4^{2-} and other

sulfonate-containing anions can support significant voltage sensitivity of prestin. The active role of SO_4^{2-} may not seem unreasonable since protein database comparisons indicate that prestin shows homology to sulfate transporters (Zheng *et al.* 2001). Nevertheless, we performed tests to rule out possible contamination of our solutions with other known active anions, namely the halides and nitrate. Independent laboratory (Galbraith Labs, TN, USA) tests indicate that these anions were less than 100–200 μM in our solutions. Additionally, we confirmed even lower Cl^- levels by measuring junction potentials at the Ag–AgCl pipette solution interface. Furthermore, bicarbonate, whose K_d for prestin effects is 44 mM (Oliver *et al.* 2001), is unlikely to be influential for several reasons. First, carbonic anhydrase is not located at the lateral wall but at the apical and basal ends of the OHC (Okamura *et al.* 1996); thus, under our conditions, the little bicarbonate that might be produced in the absence of energy substrates (i.e. in the absence of robust CO_2 generation) would be readily washed out from the cell's cytosol during pipette perfusion. Second, a control series of experiments in the presence of acetazolamide, a carbonic anhydrase inhibitor, performed in the absence of atmospheric CO_2 (using lithium hydroxide absorption), left our results unchanged (data not shown). Thus we are sure that contaminants are not responsible for our results, since, according to Oliver *et al.* (2001), at these levels of active anions non-linear capacitance should be miniscule.

Apart from differences in animal species, the membrane preparations used could be responsible for discrepancies between our data and those of Oliver *et al.* (2001) on the sulfate sensitivity of prestin. While it is certainly true that the isolated patch technique as used by Oliver *et al.* (2001) is a good method to control solutions delivered to the inner aspect of the membrane, potential problems may arise. For example, removal of a patch from a cell, or measurement of an attached patch in a transfected cell will drastically alter membrane structure, not to mention the intracellular environment that a transmembrane protein normally experiences (Milton & Caldwell, 1990). How this affects an integral membrane protein is difficult to assess. For example, both cell-attached and excised patches of oocyte-expressed Shaker-IR channels display anomalous mechanical sensitivity because normal cellular mechano-control mechanisms are absent (Gu *et al.* 2001). We have chosen to use the native, whole-cell approach because we are trying to understand how the intact cell functions. We conclude that we do have control over solutes delivered to the intracellular aspect of the lateral sub-plasmalemmal space (LSpS), at least at steady state. This, we are sure of because we find washout rates of Cl^- (based on prestin activity) typical for whole-cell washout (~1–3 min; (Pusch & Neher, 1988)); indeed, we have perfused for longer than 4 h and our results remain consistent. So, in the presence of the lateral membrane conductance that we find, the continuous perfusion of Cl^--free intracellular and extracellular solutions will eventually deplete Cl^- in the LSpS. Reversal potentials also indicate that we can effectively change LSpS Cl^- concentrations.

Allosteric effects on motor state. Oliver *et al.* (2001) suggested that extrinsic anions serve as the voltage sensor for prestin. Our data lead us to a differing view. The major effect of Cl^- is to shift the voltage operating range or state probability function of prestin along the voltage axis. The sensitivity of the operating range to Cl^- is remarkably similar to that of the ClC-0 channel (Pusch *et al.* 1995; Chen & Miller, 1996). State probability of that Cl^- channel is highly Cl^- dependent, showing a 40–50 mV change in the open probability function per 10-fold change in Cl^- concentration. We find a similar sensitivity to Cl^- concentration for prestin. In the case of ClC-0, this Cl^- sensitivity and the Cl^- ion requirement for gating have led to a consensus that the extrinsic ion serves as the voltage sensor of the channel; the channel maintains only slight residual voltage dependence under Cl^- -free conditions. Our data do not support a similar conclusion for prestin, since we find substantial voltage dependence under Cl^--free conditions, with voltage sensitivity (z) and charge movement (Q_{max}) only partially affected, and dependent upon control anion species. Additionally, if prestin required an external anionic voltage sensor, the charge movement characteristics in the presence of SO_4^{2-} and absence of Cl^- should differ significantly, with z and Q_{max} doubling owing to the change in sensor valence from −1 to −2. Thus, we conclude that the effect of Cl^- is probably due to an allosteric action on the motor protein, prestin. That is, as is typical of indirect allosteric interactions (Monod *et al.* 1963; Changeux & Edelstein, 1998), a modulator, in this case Cl^-, binds to a site (sites) that is distinct from the active site (sites) responsible for the main function of the protein, namely the intrinsically charged voltage-sensing moiety. The binding produces a reversible conformational change in prestin that changes the free energy minima of the steady-state energy profile. This we measure as a shift in the motor charge's Boltzmann function along the voltage axis. Allosteric modulation such as this is not unusual. For example, allosteric modulation of the HERG potassium channel by Ca^{2+} induces voltage shifts in the activation curve of the channel (Johnson *et al.* 2001).

Effect of Cl^- on area state of prestin. We showed that pentane sulfonate has direct effects on the OHC motor, depressing the motor's voltage sensitivity (z) much as salicylate does (Kakehata & Santos-Sacchi, 1996), while maintaining near normal Q_{max}. Indeed, as with salicylate, we still observe reduced electromotility, in contrast to the results of Oliver *et al.* (2001). Additionally, the shift of V_{pkcm} with pentane sulfonate solutions is opposite to that of our other control anions, sulfate or Hepes. We suspect that the lipophilic pentane side chain allows this organic

anion to work on normally inaccessible sites within the lipid environment of the motor, and its use does not allow an adequate evaluation of the effect of chloride on the charge or mechanical activity of prestin.

Oliver *et al.* (2001) concluded that removal of intracellular Cl^- causes the lateral membrane motor to reside in the contracted state, and consequently modelled prestin as expanding following the binding and translocation of intracellular Cl^- to the outer aspect of the membrane. However, this is unlikely because the state probability of the motor at a fixed holding voltage depends directly on the relative position of V_{pkcm}. Since we clearly show that the effects of pentane sulfate are unrelated to intracellular Cl^- concentration, their results probably reflect not the removal of Cl^-, but the negative shift of V_{pkcm} produced by pentane sulfonate, which they exclusively used in their motility studies. We find that with sulfate- or Hepes-based solutions, where the effects we observe actually correspond to the removal of Cl^-, the motors tend to reside in the expanded state with Cl^- removal, i.e. the OHC elongates at a fixed holding potential, as V_{pkcm} shifts in the positive direction. Thus, we conclude that the binding of Cl^- to prestin actually increases the probability that the protein resides in the contracted state and it is unlikely that binding and movement of the negatively charged Cl^- ion towards the outer membrane leaflet would increase prestin surface area as Oliver *et al.* (2001) modelled. We suggest that upon Cl^- binding, prestin activity is shifted into the physiological range of voltages where intrinsic charge may sense voltage perturbation. Contraction of prestin would be caused by a moiety of net positive charge moving outward, or one of net negative charge moving inward as the electrophysiological data suggests (Ashmore, 1990; Santos-Sacchi, 1991*b*).

How many prestin binding sites are there for anions? We find differential changes in V_{pkcm}, z and Q_{max} that depend on the control anions (sulfate or Hepes) that we use to replace Cl^-. This observation indicates that multiple populations of anion-bound prestin may exist simultaneously, and we hypothesize that there are multiple binding sites that can bind not only Cl^- but other anions with different affinities, each having differential effects on the Boltzmann parameters. For the whole cell, and large patches, we must also be cognisant that still other restricted populations of motors (with different Boltzmann characteristics) may also exist as a result of local forces other than Cl^-, e.g. tension, phosphorylation (Santos-Sacchi, 2002). Consequently, owing to distributed populations, the resulting single Boltzmann distributions that we observe do not demonstrate any apparent discontinuities.

Flux of Cl^- through the lateral membrane

Identity of the lateral membrane conductance. In this report we directly measured voltage- and stretch-activated anionic and cationic currents that arise from a lateral membrane conductance, and confirmed Cl^- movements by monitoring non-linear capacitance. Several lines of evidence indicate that these non-selective currents, hereafter referred to as I_{metL} (mechano–electrical transducer, lateral membrane), pass through the same conductance: (1) the anionic and cationic currents co-vary in magnitude among OHCs, and never exist separately; each of the magnitudes proportionately fluctuates among and within cells; (2) all modulating agents (drugs, turgor pressure) affect each current in the same direction, and with approximately equal effects; (3) each shows identical rapid kinetics and sigmoidal voltage dependence; and (4) the currents localize to the lateral plasma membrane, being absent in plasma membrane lacking prestin, namely, at the OHC base and in supporting cells.

The number of ionic conductances that are known to exist in the OHC is growing. Some have been molecularly identified and physiologically characterized, e.g. the KCNQ channel subunits responsible for the $I_{k,n}$ current (Kubisch *et al.* 1999; Marcotti & Kros, 1999), or functionally linked to a particularly well characterized channel type, e.g. the L-type Ca^{2+} channel (Santos-Sacchi & Dilger, 1988; Nakagawa *et al.* 1991). Others have been identified through the detection of messenger RNA, e.g. ClC family members (Kawasaki *et al.* 1999), but lack corresponding physiological confirmation of expression. There are still others that have been highly characterized but whose molecular identity remains elusive after decades of study, e.g. the stereocilia transduction channel (Russell *et al.* 1989; Kros *et al.* 1992). Although the molecular identity of the conductance responsible for I_{metL} is unknown, its unusual characteristics are not unprecedented. Indeed, a poorly charge-selective, stretch-sensitive conductance that passes Na^+, K^+ and Cl^- has been characterized at the single channel level in opossum kidney cells (Ubl *et al.* 1988).

The major voltage-dependent ionic conductances of the OHC, including outward K^+ and inward Ca^{2+}, are restricted to the basal pole of the cell (Santos-Sacchi *et al.* 1997). Though it is generally accepted that the predominant constituent of the lateral membrane is the motor protein, prestin, ionic conductances other than the one we have characterized are localized to this region. Notably, stretch-activated channels have been found in the lateral membrane of OHCs, though they are selective for cations (Ding *et al.* 1991; Iwasa *et al.* 1991), and clearly could not account for the anionic currents that we observed. Brownell and colleagues have observed stretch-induced pore formation up to 4 nm in size in the OHC membrane, which is inhibited by chlorpromazine (Morimoto *et al.* 2002). They found that the pores passed mono and disaccharides, though the ionic permeability of these pores has not been elucidated. Interestingly, there are some reports that may have observed the effects of I_{metL} on OHC shape. Notably, tamoxifen and quinine have been shown to block swelling of OHCs in cochlear explants (Siegel *et al.* 2001), and Gd^{3+}

was found to interfere with volume regulation in isolated OHCs (Crist *et al.* 1993). It was suggested that tamoxifen had its effect on ClC-3 channels in OHCs (Siegel *et al.* 2001). Our data do not support this.

Finally, we note that I_{metL} shares some properties of prestin, namely, its location, tension dependence, and modulation by Cl^- channel blockers. In this regard, it is well established that some transporters underlie ionic conductances, including CFTR (Hasegawa *et al.* 1992) and the sodium/bicarbonate co-transporter, NBCn1 (Choi *et al.* 2000). In fact, the Na^+ current associated with NBCn1 expression shows an increase in response to DIDS (Choi *et al.* 2000), similar to the activity of this blocker on I_{metL}. It is conceivable that I_{metL} could result from the expression of prestin. Nevertheless, regardless of the conductance's molecular identity, it is clear that it has a major impact on the activity of prestin and the OHC.

Sub-membranous Cl^-. I_{metL} is localized to the lateral plasma membrane of the OHC. The lateral membrane and subsurface cisternae form membranous barriers of a restricted compartment (LSpS) whose diffusional access to and from the cytosol is limited owing to its ~30 nm width (Pollice & Brownell, 1993). The LSpS may have distinctive properties (Halter *et al.* 1997; Ratnanather *et al.* 2000). As the cistern nearest the plasma membrane is continuous, ion diffusion must predominantly occur at the apical and basal extremes of the OHC, where the cisternae terminate. For the isolated cells we used in the present study, with lengths from 50 to 80 μm, the volume of the LSpS is about 47–66 fl. If washout from the bulk cytosol under whole-cell voltage clamp were completely absent, the magnitude of I_{metL} we observed, for example ~100 pA at −60 mV (see Fig. 10*A*), would change LSpS Cl^- levels at a rate of 20 mM s^{-1}. Actually, the concentration change just beneath the plasma membrane and at high frequencies (owing to diffusion-rate limitations), especially in the middle of the cell, could be substantially larger. This may explain to some extent our observation of non-uniform stretch-activated gating currents along the length of the OHCs, as non-linear capacitance magnitude will vary with Cl^- concentration (Takahashi & Santos-Sacchi, 2001). Since we find that intracellular dialysis with Cl^--free solutions affects prestin activity with a time course typical for whole-cell washout (Pusch & Neher, 1988), it is clear that LSpS is not absolutely isolated, and thus, Cl^- levels in that space are under our experimental control, at least at steady state (> 3 min). Nevertheless, reversal potential measures indicate substantial gradients in concentration between core cytosol and LSpS. Under whole-cell voltage clamp, the concentration of Cl^- in the LSpS is a balance between intracellular/LSpS diffusion and flux across the lateral plasma membrane. Clearly, then, in the absence of Cl^--containing solutions inside and outside the cell for more than several minutes we are assured that Cl^- is depleted in the LSpS, and the conclusions that we reached based on this result, e.g. that Q_{max} is resistant to Cl^- depletion, are valid.

Under normal physiological conditions, other homeostatic mechanisms to control Cl^- levels may come into play, for example, pumps, transporters and sequestration mechanisms (see Frings *et al.* 2000), just as they do in calcium metabolism. Most cells maintain an intracellular Cl^- concentration that is substantially below the typical extracellular concentration of 140 mM, as in perilymph. Nevertheless, in many cell types Cl^- is maintained at levels higher than the predicted electrochemical equilibrium levels. This is usually achieved by Na^+–K^+–2Cl^- cotransport (Russell, 2000). However, there is an apparent absence of NKCC1 transporter in OHCs (Crouch *et al.* 1997; Goto *et al.* 1997); this may indicate that levels in the OHC are close to equilibrium levels, namely, for a resting potential < −70 mV (Dallos *et al.* 1982), Cl^- would be < 9 mM. Furthermore, efficient mechanisms for the control of Cl^- must exist within the very localized region of the LSpS, since an incessant flux of Cl^- across the lateral membrane is predicted to accompany acoustically induced (or basilar membrane vibration-induced) mechanical deformations of the cell. As noted above, changes in Cl^- levels in the LSpS will have a strong impact on OHC mechanical function. We speculate that the subsurface cisternae and associated mitochondria aid in controlling LSpS Cl^- levels. Indeed, it may be that interference with Cl^- homeostatic mechanisms underlies the susceptibility of the cochlear amplifier to trauma, or that modulation of these mechanisms accounts for normal phenomenon such as the shift in V_{pkcm} observed during OHC development (Oliver & Fakler, 1999).

Physiological implications of a fast stretch-activated lateral membrane Cl^- current – a hypothesis

The observation that OHC somatic motility is driven by voltage quickly led to the suggestion that the low-pass filter of the membrane would seriously limit high frequency electromotility (Santos-Sacchi, 1989). This problem only arises when one considers that owing to the non-linear nature of the mechanical response function, the mechanical gain of the OHC is about one tenth of its maximum (max: ~30 nm mV^{-1}) at the normal resting potential of −70 mV (Santos-Sacchi, 1989). Since that observation, a few solutions for the apparent RC filter problem have been suggested. Dallos & Evans (1995) suggested a mechanism that may work in the intact cochlea; during stimulation with high acoustic frequencies, extracellular voltages (which have a wider bandwidth than intracellular potentials) deriving from excited OHCs could induce a voltage drop across unexcited OHCs at basilar membrane regions basal to the excited cell region. Alternatively, we have suggested two cellular-based mechanisms whereby the problem could be alleviated. First, we found that the mechanical

gain of the cell at its resting potential could be increased via reductions in turgor pressure (Kakehata & Santos-Sacchi, 1995). Second, since we found that motor charge density is greater in higher frequency OHCs, we reasoned that the resultant electrical energy ($Q \times V$) delivered to the lateral membrane of high frequency OHCs could render the filter-induced drop in receptor potentials less detrimental (Santos-Sacchi *et al.* 1998*a*). All these arguments presuppose the existence of an RC filter problem due to voltage dependence of prestin. Our new data identify a potential mechanism for the operation of the cochlear amplifier without RC filter problems.

The identification of a stretch-activated conductance (G_{metL}) in the lateral membrane may indicate that the OHC motor can react to currents evoked by mechanical perturbations that accompany acoustic stimulation *in vivo*. This scenario had been envisioned following the discovery of stretch-activated cationic channels in the lateral membrane (Ding *et al.* 1991; Iwasa *et al.* 1991). Under that scheme, voltage perturbations accompanying the flux of cations were suggested to drive the OHC motor. However, in that case the RC filter problem remained. In our hypothetical view, however, Cl^- oscillations near prestin, driven by the stretch-activated AC and/or DC Cl^- current component of I_{metL}, would directly drive prestin transitions. This mechanism naturally follows from the substantial influence of Cl^- on the state probability of prestin. As the current or its integral, not the resultant voltage, would directly modulate prestin, the mechanism would be unencumbered by the RC membrane filter. Thus, we hypothesise that the OHC soma has adopted a mechanism similar to that which stereocilia may use to provide cochlear amplification in lower vertebrates (Choe *et al.* 1998; Ricci *et al.* 2000). In that case, Ca^{2+} ion entry through the mechanically gated transduction channels modulates the channels themselves and thus stereocilia bundle mechanics (Choe *et al.* 1998; Ricci *et al.* 2000). In an analogous manner, we view the lateral membrane as a forward and reverse transducer, where local changes in intracellular Cl^- levels lead to a cyclical binding of Cl^- to prestin, with resultant changes in OHC mechanical properties. Obviously, to be functional, the lateral membrane model must meet many of the requirements laid out for models of stereocilia amplification (Choe *et al.* 1998), including the need for rapid association and dissociation rate constants and mechanisms for Cl^- removal.

If this hypothesis has merit, then extracellular perilymphatic Cl^- levels should be important for normal auditory function. Manipulations of perilymphatic Cl^- levels have been made, but the results are not clear cut (Desmedt & Robertson, 1975). Regarding the interpretation of perilymphatic perfusion of any type, we must remain cognisant of the possibility that preparation for these kinds of experiments can sometimes reduce response levels significantly such that threshold (active) effects can be missed. Indeed, Desmedt & Robertson (1975) described their preparations as 'fairly intact', and found variations of up to 20 % in cochlear microphonic (CM) and eighth nerve compound action potential (N1) thresholds during control perfusions. Nevertheless, when low Cl^- perilymphatic-perfusion rates were increased so as to drop Cl^- levels down to 5 mM, N1 threshold levels did deteriorate, as we would predict.

REFERENCES

Aickin CC & Brading AF (1984). The role of chloride–bicarbonate exchange in the regulation of intracellular chloride in guinea-pig vas deferens. *J Physiol* **349**, 587–606.

Allen MC, Newland C, Valverde MA & Hardy SP (1998). Inhibition of ligand-gated cation-selective channels by tamoxifen. *Eur J Pharmacol* **354**, 261–269.

Ashmore JF (1986). The cellular physiology of isolated outer hair cells: implications for cochlear frequency selectivity. In *Auditory Frequency Selectivity*, ed. Moore BC & Patterson RD, pp. 103–108. Plenum Press, New York.

Ashmore JF (1987). A fast motile response in guinea-pig outer hair cells: the cellular basis of the cochlear amplifier. *J Physiol* **388**, 323–347.

Ashmore JF (1989). Transducer motor coupling in cochlear outer hair cells. In *Mechanics of Hearing,* ed. Kemp D & Wilson JP, pp. 107–113. Plenum Press, New York.

Ashmore JF (1990). Forward and reverse transduction in the mammalian cochlea. *Neurosci Res Suppl* **12**, S39–50.

Ashmore JF & Meech RW (1986). Ionic basis of membrane potential in outer hair cells of guinea pig cochlea. *Nature* **322**, 368–371.

Belyantseva I, Adler HJ, Curi R, Frolenkov GI & Kachar B (2000*a*). Expression and localization of prestin and the sugar transporter GLUT-5 during development of electromotility in cochlear outer hair cells. *J Neurosci* **20**, RC116.

Belyantseva IA, Frolenkov GI, Wade JB, Mammano F & Kachar B (2000*b*). Water permeability of cochlear outer hair cells: characterization and relationship to electromotility. *J Neurosci* **20**, 8996–9003.

Brownell WE, Bader CR, Bertrand D & de Ribaupierre Y (1985). Evoked mechanical responses of isolated cochlear outer hair cells. *Science* **227**, 194–196.

Brundin L, Flock A & Canlon B (1989). Sound-induced motility of isolated cochlear outer hair cells is frequency-specific. *Nature* **342**, 814–816.

Brundin L & Russell I (1994). Tuned phasic and tonic motile responses of isolated outer hair cells to direct mechanical stimulation of the cell body. *Hear Res* **73**, 35–45.

Changeux JP & Edelstein SJ (1998). Allosteric receptors after 30 years. *Neuron* **21**, 959–980.

Chen TY & Miller C (1996). Nonequilibrium gating and voltage dependence of the ClC-0 Cl^- channel. *J Gen Physiol* **108**, 237–250.

Choe Y, Magnasco MO & Hudspeth AJ (1998). A model for amplification of hair-bundle motion by cyclical binding of Ca^{2+} to mechanoelectrical-transduction channels. *Proc Natl Acad Sci U S A* **95**, 15321–15326.

Choi I, Aalkjaer C, Boulpaep EL & Boron WF (2000). An electroneutral sodium/bicarbonate cotransporter NBCn1 and associated sodium channel. *Nature* **405**, 571–575.

Crist JR, Fallon M & Bobbin RP (1993). Volume regulation in cochlear outer hair cells. *Hear Res* **69**, 194–198.

Crouch JJ, Sakaguchi N, Lytle C & Schulte BA (1997). Immunohistochemical localization of the Na–K–Cl co-transporter (NKCC1) in the gerbil inner ear. *J Histochem Cytochem* **45**, 773–778.

Dallos P (1992). The active cochlea. *J Neurosci* **12**, 4575–4585.

Dallos P & Evans BN (1995). High-frequency outer hair cell motility: corrections and addendum. *Science* **268**, 1420–1421.

Dallos P, Evans BN & Hallworth R (1991). Nature of the motor element in electrokinetic shape changes of cochlear outer hair cells. *Nature* **350**, 155–157.

Dallos P & Santos-Sacchi J (1983). AC receptor potentials from hair cells in the low frequency region of the guinea pig cochlea. In *Mechanisms of Hearing*, ed. Webster WR & Aitkin LM, pp. 11–16. Monash University Press, Clayton, Australia.

Dallos P, Santos-Sacchi J & Flock A (1982). Intracellular recordings from cochlear outer hair cells. *Science* **218**, 582–584.

Desmedt JE & Robertson D (1975). Ionic mechanism of the efferent olivo-cochlear inhibition studied by cochlear perfusion in the cat. *J Physiol* **247**, 407–428.

Ding JP, Salvi RJ & Sachs F (1991). Stretch-activated ion channels in guinea pig outer hair cells. *Hear Res* **56**, 19–28.

Draguhn A, Traub RD, Schmitz D & Jefferys JG (1998). Electrical coupling underlies high-frequency oscillations in the hippocampus *in vitro*. *Nature* **394**, 189–192.

Frank G, Hemmert W & Gummer AW (1999). Limiting dynamics of high-frequency electromechanical transduction of outer hair cells. *Proc Natl Acad Sci U S A* **96**, 4420–4425.

Frazier CJ, George EG & Jones SW (2000). Apparent change in ion selectivity caused by changes in intracellular K(+) during whole-cell recording. *Biophys J* **78**, 1872–1880.

Frings S, Reuter D & Kleene SJ (2000). Neuronal Ca^{2+}-activated Cl^- channels – homing in on an elusive channel species. *Prog Neurobiol* **60**, 247–289.

Gale JE & Ashmore JF (1994). Charge displacement induced by rapid stretch in the basolateral membrane of the guinea-pig outer hair cell. *Proc R Soc Lond* B *Biol Sci* **255**, 243–249.

Goto S, Oshima T, Ikeda K, Ueda N & Takasaka T (1997). Expression and localization of the Na–K–2Cl cotransporter in the rat cochlea. *Brain Res* **765**, 324–326.

Gu CX, Juranka PF & Morris CE (2001). Stretch-activation and stretch-inactivation of Shaker-IR, a voltage-gated K^+ channel. *Biophys J* **80**, 2678–2693.

Gunthorpe MJ, Benham CD, Randall A & Davis JB (2002). The diversity in the vanilloid (TRPV) receptor family of ion channels. *Trends Pharmacol Sci* **23**, 183–191.

Halter JA, Kruger RP, Yium MJ & Brownell WE (1997). The influence of the subsurface cisterna on the electrical properties of the outer hair cell. *NeuroReport* **8**, 2517–2521.

Hasegawa H, Skach W, Baker O, Calayag MC, Lingappa V & Verkman AS (1992). A multifunctional aqueous channel formed by CFTR. *Science* **258**, 1477–1479.

Huang G & Santos-Sacchi J (1993). Mapping the distribution of the outer hair cell motility voltage sensor by electrical amputation. *Biophys J* **65**, 2228–2236.

Iwasa KH (1993). Effect of stress on the membrane capacitance of the auditory outer hair cell. *Biophys J* **65**, 492–498.

Iwasa KH (1994). A membrane motor model for the fast motility of the outer hair cell. *J Acoust Soc Am* **96**, 2216–2224.

Iwasa KH & Kachar B (1989). Fast *in vitro* movement of outer hair cells in an external electric field: effect of digitonin, a membrane permeabilizing agent. *Hear Res* **40**, 247–254.

Iwasa KH, Li MX, Jia M & Kachar B (1991). Stretch sensitivity of the lateral wall of the auditory outer hair cell from the guinea pig. *Neurosci Lett* **133**, 171–174.

Jentsch TJ, Stein V, Weinreich F & Zdebik AA (2002). Molecular structure and physiological function of chloride channels. *Physiol Rev* **82**, 503–568.

Johnson JP Jr, Balser JR & Bennett PB (2001). A novel extracellular calcium sensing mechanism in voltage-gated potassium ion channels. *J Neurosci* **21**, 4143–4153.

Kachar B, Brownell WE, Altschuler R & Fex J (1986). Electrokinetic shape changes of cochlear outer hair cells. *Nature* **322**, 365–368.

Kakehata S & Santos-Sacchi J (1995). Membrane tension directly shifts voltage dependence of outer hair cell motility and associated gating charge. *Biophys J* **68**, 2190–2197.

Kakehata S & Santos-Sacchi J (1996). Effects of salicylate and lanthanides on outer hair cell motility and associated gating charge. *J Neurosci* **16**, 4881–4889.

Kalinec F, Holley MC, Iwasa KH, Lim DJ & Kachar B (1992). A membrane-based force generation mechanism in auditory sensory cells. *Proc Natl Acad Sci U S A* **89**, 8671–8675.

Kawasaki E, Hattori N, Miyamoto E, Yamashita T & Inagaki C (1999). Single-cell RT-PCR demonstrates expression of voltage-dependent chloride channels (ClC-1, ClC-2 and ClC-3) in outer hair cells of rat cochlea. *Brain Res* **838**, 166–170.

Kros CJ, Rusch A & Richardson GP (1992). Mechano-electrical transducer currents in hair cells of the cultured neonatal mouse cochlea. *Proc R Soc Lond* B *Biol Sci* **249**, 185–193.

Kubisch C, Schroeder BC, Friedrich T, Lutjohann B, El Amraoui A, Marlin S, Petit C & Jentsch TJ (1999). KCNQ4, a novel potassium channel expressed in sensory outer hair cells, is mutated in dominant deafness. *Cell* **96**, 437–446.

Liberman MC, Gao J, He DZZ, Wu XD, Jia SP & Zuo J (2002). Prestin is required for electromotility of the outer hair cell and for the cochlea amplifier. *Nature* **419**, 300–304.

Ludwig J, Oliver D, Frank G, Klocker N, Gummer AW & Fakler B (2001). Reciprocal electromechanical properties of rat prestin: The motor molecule from rat outer hair cells. *Proc Natl Acad Sci U S A* **98**, 4178–4183.

Marcotti W & Kros CJ (1999). Developmental expression of the potassium current $I_{K,n}$ contributes to maturation of mouse outer hair cells. *J Physiol* **520**, 653–660.

Milton RL & Caldwell JH (1990). How do patch clamp seals form? A lipid bleb model. *Pflugers Arch* **416**, 758–762.

Monod J, Changeux JP & Jacob F (1963). Allosteric proteins and cellular control systems. *J Mol Biol* **6**, 306–329.

Morimoto N, Raphael RM, Nygren A & Brownell WE (2002). Excess plasma membrane and effects of ionic amphipaths on mechanics of outer hair cell lateral wall. *Am J Physiol Cell Physiol* **282**, C1076–1086.

Nakagawa T, Kakehata S, Akaike N, Komune S, Takasaka T & Uemura T (1991). Calcium channel in isolated outer hair cells of guinea pig cochlea. *Neurosci Lett* **125**, 81–84.

Okamura HO, Sugai N, Suzuki K & Ohtani I (1996). Enzyme-histochemical localization of carbonic anhydrase in the inner ear of the guinea pig and several improvements of the technique. *Histochem Cell Biol* **106**, 425–430.

Oliver D & Fakler B (1999). Expression density and functional characteristics of the outer hair cell motor protein are regulated during postnatal development in rat. *J Physiol* **519**, 791–800.

Oliver D, He DZ, Klocker N, Ludwig J, Schulte U, Waldegger S, Ruppersberg JP, Dallos P & Fakler B (2001). Intracellular anions as the voltage sensor of prestin, the outer hair cell motor protein. *Science* **292**, 2340–2343.

Pollice PA & Brownell WE (1993). Characterization of the outer hair cell's lateral wall membranes. *Hear Res* **70**, 187–196.

Pusch M, Ludewig U, Rehfeldt A & Jentsch TJ (1995). Gating of the voltage-dependent chloride channel CIC-0 by the permeant anion. *Nature* **373**, 527–531.

Pusch M & Neher E (1988). Rates of diffusional exchange between small cells and a measuring patch pipette. *Pflugers Arch* **411**, 204–211.

Ratnanather JT, Popel AS & Brownell WE (2000). An analysis of the hydraulic conductivity of the extracisternal space of the cochlear outer hair cell. *J Math Biol* **40**, 372–382.

Ricci AJ, Crawford AC & Fettiplace R (2000). Active hair bundle motion linked to fast transducer adaptation in auditory hair cells. *J Neurosci* **20**, 7131–7142.

Ruggero MA & Rich NC (1991). Furosemide alters organ of corti mechanics: evidence for feedback of outer hair cells upon the basilar membrane. *J Neurosci* **11**, 1057–1067.

Russell IJ, Richardson GP & Kossl M (1989). The responses of cochlear hair cells to tonic displacements of the sensory hair bundle. *Hear Res* **43**, 55–69.

Russell JM (2000). Sodium–potassium–chloride cotransport. *Physiol Rev* **80**, 211–276.

Rybalchenko & Santos-Sacchi (2001) Modulation of outer hair cell capacitance by chloride ions. *Inner Ear Biology Meeting Abstracts*, Rome, Italy, September 2001. http://ieb.unife.it/ieb2001/abstracts/cell_signalling.html

Santos-Sacchi J (1989). Asymmetry in voltage-dependent movements of isolated outer hair cells from the organ of Corti. *J Neurosci* **9**, 2954–2962.

Santos-Sacchi J (1991*a*). Isolated supporting cells from the organ of Corti: some whole cell electrical characteristics and estimates of gap junctional conductance. *Hear Res* **52**, 89–98.

Santos-Sacchi J (1991*b*). Reversible inhibition of voltage-dependent outer hair cell motility and capacitance. *J Neurosci* **11**, 3096–3110.

Santos-Sacchi J (1992). On the frequency limit and phase of outer hair cell motility: effects of the membrane filter. *J Neurosci* **12**, 1906–1916.

Santos-Sacchi J (1993). Harmonics of outer hair cell motility. *Biophys J* **65**, 2217–2227.

Santos-Sacchi J (2002). Functional motor microdomains of the outer hair cell lateral membrane. *Pflugers Arch* **445**, 331–336.

Santos-Sacchi J & Dilger JP (1988). Whole cell currents and mechanical responses of isolated outer hair cells. *Hear Res* **35**, 143–150.

Santos-Sacchi J, Huang GJ & Wu M (1997). Mapping the distribution of outer hair cell voltage-dependent conductances by electrical amputation. *Biophys J* **73**, 1424–1429.

Santos-Sacchi J, Kakehata S, Kikuchi T, Katori Y & Takasaka T (1998*a*). Density of motility-related charge in the outer hair cell of the guinea pig is inversely related to best frequency. *Neurosci Lett* **256**, 155–158.

Santos-Sacchi J, Kakehata S & Takahashi S (1998*b*). Effects of membrane potential on the voltage dependence of motility-related charge in outer hair cells of the guinea-pig. *J Physiol* **510**, 225–235.

Santos-Sacchi J & Navarrete E (2002). Voltage-dependent changes in specific membrane capacitance caused by prestin, the outer hair cell lateral membrane motor. *Pflugers Arch* **444**, 99–106.

Santos-Sacchi J, Shen W, Zheng J & Dallos P (2001). Effects of membrane potential and tension on prestin, the outer hair cell lateral membrane motor protein. *J Physiol* **531**, 661–666.

Siegel J, Sikka R, Zeddies DG & Dong Q (2001). Intact explanted adult gerbil cochleae maintained at body temperature. *Assoc Res Otolaryngol Abs*, p. 240.

Takahashi S & Santos-Sacchi J (2001). Non-uniform mapping of stress-induced, motility-related charge movement in the outer hair cell plasma membrane. *Pflugers Arch* **441**, 506–513.

Thoreson WB, Nitzan R & Miller RF (2000). Chloride efflux inhibits single calcium channel open probability in vertebrate photoreceptors: chloride imaging and cell-attached patch-clamp recordings. *Vis Neurosci* **17**, 197–206.

Ubl J, Murer H & Kolb HA (1988). Ion channels activated by osmotic and mechanical stress in membranes of opossum kidney cells. *J Membr Biol* **104**, 223–232.

Welsh DG, Nelson MT, Eckman DM & Brayden JE (2000). Swelling-activated cation channels mediate depolarization of rat cerebrovascular smooth muscle by hyposmolarity and intravascular pressure. *J Physiol* **527**, 139–148.

Yang XC & Sachs F (1989). Block of stretch-activated ion channels in *Xenopus* oocytes by gadolinium and calcium ions. *Science* **243**, 1068–1071.

Zhao HB & Santos-Sacchi J (1999). Auditory collusion and a coupled couple of outer hair cells. *Nature* **399**, 359–362.

Zheng J, Long KB, Shen W, Madison LD & Dallos P (2001). Prestin topology: localization of protein epitopes in relation to the plasma membrane. *NeuroReport* **12**, 1929–1935.

Zheng J, Shen W, He D, Long K, Madison L & Dallos P (2000). Prestin is the motor protein of cochlear outer hair cells. *Nature* **405**, 149–155.

Acknowledgements

We thank Chris Miller and Fred Sachs for helpful discussions and Margaret Mazzucco for technical help. This study was supported by NIH NIDCD DC00273.